NCHRP Web Document 68 (Project 9-27)

Relationships of HMA In-Place Air Voids, Lift Thickness, and Permeability
Volume Two

Prepared for:

National Cooperative Highway Research Program

TRANSPORTATION RESEARCH BOARD
OF THE NATIONAL ACADEMIES

Submitted by:

E. Ray Brown
M. Rosli Hainin
Allen Cooley
Graham Hurley
National Center for Asphalt Technology
Auburn University
Auburn, Alabama

September 2004

ACKNOWLEDGMENT

This work was sponsored by the American Association of State Highway and Transportation Officials (AASHTO), in cooperation with the Federal Highway Administration, and was conducted in the National Cooperative Highway Research Program (NCHRP), which is administered by the Transportation Research Board (TRB) of the National Academies.

THE NATIONAL ACADEMIES

Advisers to the Nation on Science, Engineering, and Medicine

The **National Academy of Sciences** is a private, nonprofit, self-perpetuating society of distinguished scholars engaged in scientific and engineering research, dedicated to the furtherance of science and technology and to their use for the general welfare. On the authority of the charter granted to it by the Congress in 1863, the Academy has a mandate that requires it to advise the federal government on scientific and technical matters. Dr. Bruce M. Alberts is president of the National Academy of Sciences.

The **National Academy of Engineering** was established in 1964, under the charter of the National Academy of Sciences, as a parallel organization of outstanding engineers. It is autonomous in its administration and in the selection of its members, sharing with the National Academy of Sciences the responsibility for advising the federal government. The National Academy of Engineering also sponsors engineering programs aimed at meeting national needs, encourages education and research, and recognizes the superior achievements of engineers. Dr. William A. Wulf is president of the National Academy of Engineering.

The **Institute of Medicine** was established in 1970 by the National Academy of Sciences to secure the services of eminent members of appropriate professions in the examination of policy matters pertaining to the health of the public. The Institute acts under the responsibility given to the National Academy of Sciences by its congressional charter to be an adviser to the federal government and, on its own initiative, to identify issues of medical care, research, and education. Dr. Harvey V. Fineberg is president of the Institute of Medicine.

The **National Research Council** was organized by the National Academy of Sciences in 1916 to associate the broad community of science and technology with the Academy's purposes of furthering knowledge and advising the federal government. Functioning in accordance with general policies determined by the Academy, the Council has become the principal operating agency of both the National Academy of Sciences and the National Academy of Engineering in providing services to the government, the public, and the scientific and engineering communities. The Council is administered jointly by both the Academies and the Institute of Medicine. Dr. Bruce M. Alberts and Dr. William A. Wulf are chair and vice chair, respectively, of the National Research Council.

The **Transportation Research Board** is a division of the National Research Council, which serves the National Academy of Sciences and the National Academy of Engineering. The Board's mission is to promote innovation and progress in transportation through research. In an objective and interdisciplinary setting, the Board facilitates the sharing of information on transportation practice and policy by researchers and practitioners; stimulates research and offers research management services that promote technical excellence; provides expert advice on transportation policy and programs; and disseminates research results broadly and encourages their implementation. The Board's varied activities annually engage more than 5,000 engineers, scientists, and other transportation researchers and practitioners from the public and private sectors and academia, all of whom contribute their expertise in the public interest. The program is supported by state transportation departments, federal agencies including the component administrations of the U.S. Department of Transportation, and other organizations and individuals interested in the development of transportation.
www.TRB.org

VOLUME TWO
TABLE OF CONTENTS

Page

LIST OF TABLES

Page

LIST OF FIGURES

CONTROLLED LABORATORY EXPERIMENT TO EVALUATE METHODS OF MEASURING THE BULK SPECIFIC GRAVITY OF COMPACTED HMA
NCHRP 9-27
TASK 3-PART 3

1.0 INTRODUCTION AND PROBLEM STATEMENT

A major concern of the hot mix asphalt (HMA) industry is the proper measurement of bulk specific gravity (G_{mb}) of compacted samples. This issue has become a bigger problem with the increased use of coarse gradations. Bulk specific gravity measurements are the basis for volumetric calculations used during HMA mix design, field control, and construction acceptance. During mix design, volumetric properties such as air voids, voids in mineral aggregates, voids filled with asphalt, and percent theoretical maximum density at a certain number of gyrations are used to evaluate the acceptability of mixes. All of these properties are based upon G_{mb}.

In most states, acceptance of HMA construction by the owner is typically based upon percent compaction calculated as a percent of theoretical maximum density. Whether nondestructive (e.g., nuclear gauges) or destructive (e.g., cores) tests are used as the basis of acceptance, G_{mb} measurements are equally important. When nondestructive devices are utilized, each device has to first be calibrated to the G_{mb} of cores. If the G_{mb} measurements of the cores are inaccurate in this calibration step, then the nondestructive device will provide inaccurate data. Additionally, pay factors for construction, whether reductions or bonuses, are generally applied to percent compaction. Thus, errors in G_{mb} measurements can potentially affect both the agency and producer.

For many years, the measurement of G_{mb} for compacted HMA has been accomplished by the water displacement method using saturated-surface dry (SSD) samples. This method consists of first weighing a dry sample in air, then obtaining a

submerged mass after the sample has been placed in a water bath for a specified time interval. Upon removal from the water bath, the SSD mass is determined after patting the sample dry using a damp towel. Procedures for this test method are outlined in AASHTO T166 and the equivalent ASTM D2726.

The SSD method has proved adequate for conventionally designed mixes, such as Marshall and Hveem methods, that generally utilized fine-graded aggregates. Historically, mixes were designed to have gradations passing close to or above the Superpave defined maximum density line (i.e., fine-graded). However, since the adoption of the Superpave mix design system and the increased use of stone matrix asphalt (SMA), mixes are being designed with coarser gradations than used in the past.

The potential problem in measuring the G_{mb} of mixes like coarse-graded Superpave and SMA using the SSD method comes from their internal air void structure. These types of mixes tend to have larger internal air voids than the finer conventional mixes at similar overall air void contents. Mixes with coarser gradations have a much higher percentage of large aggregate particles. At a certain overall air void volume, which is mix specific, the large internal air voids of the coarse mixes can become interconnected. During G_{mb} testing with the SSD method, water can quickly infiltrate into the sample through these interconnected voids. However, after removing the sample from the water bath to obtain the saturated-surface dry condition the water can also drain from the sample quickly. This draining of the water from the sample causes errors when using the SSD method.

To understand the cause of potential errors, one must first understand the principles of the SSD method. The philosophy of the SSD method is based upon

Archimedes' Principle, which states that a force equal to the mass of the displaced fluid buoys up a material immersed in fluid. Take for instance the material submerged in water illustrated within Figure 1. The surface of the material that is in contact with water can be divided into two halves: the upper surface (face BCE) and lower surface (face BDE). Submerged in this manner, there are three forces acting on the material: 1) the weight of the material in a dry condition (W_M); 2) the force of the water within ABCEF on the material (F_{D2}); and 3) the force of the buoyant resistance acting upward (F_{U1}) which is equal to the weight of water within ABDEF.

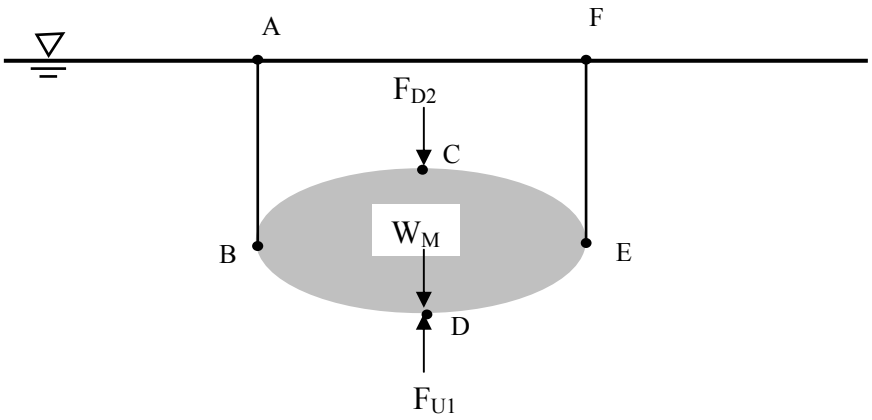

Figure 1. Hydrostatic Forces on a Submerged Material

Using these known forces acting on the material, a series of relationships can be identified:

$$\text{Total force acting downward} = F_D = W_M + F_{D2} \qquad (1)$$

$$\text{Total net force} = F_N = W_M + F_{D2} - F_{U1} \qquad (2)$$

The net force acting downward (F_N) on the sample can be determined by measuring the weight of the material when it is submerged in water (W_{MW}). Therefore, the weight of the material submerged in water is equal to the right hand side of Equation

2. Further, the difference in the weight of the two water columns (F_{D2} and F_{U1}) is equal to the weight of fluid that is displaced when the material is submerged in water (W_W). [Note F_{U1} is greater than F_{D2}, but acts in an opposite direction.] Hence:

$$W_{MW} = W_M - W_W \quad (3)$$

Now, using the properties shown in Equations 1 through 3 and the definition of density and specific gravity, the equation using water displacement for calculating a specific gravity can be derived. The definitions for density and specific gravity are as follows:

$$\gamma_M = M_M / V_M \quad (4)$$

$$G_s = \gamma_M / \gamma_W \quad (5)$$

Where:

γ = the density of an object (γ_M for material and γ_W for water);

M_M = the dry mass of a material; and

V_M = the volume of the material.

G_s = specific gravity of a material.

Since the volume of the material is equal to the volume of the water displaced by the material, substituting Equation 4 into Equation 5 yields the following:

$$G_s = M_M / M_W \quad (6)$$

Where:

M_W= mass of displaced water

The mass of a material is equal to the weight of that material divided by the acceleration caused by gravity; therefore, Equations 3 and 6 can be used to derive the equation used for determining the specific gravity of a material:

$$Gs = M_M / (M_M - M_{MW}) \quad (7)$$

Equation 7 is the method of determining the specific gravity of a material using Archimedes' Principle. However, within the context of HMA materials this equation defines a "dry" specific gravity and not the bulk specific gravity. The term dry specific gravity is used here to indicate the dry mass of the sample is utilized in the denominator of Equation 7 to calculate specific gravity. A brief discussion of the differences between the dry and bulk specific gravities of compacted HMA is necessary.

Figure 2 illustrates volumes and air voids that are associated with compacted HMA. Each of the diagrams within Figure 2 are divided into halves with a given half representing the volumes and air voids of mixes having coarse or fine gradations. The dark black line in Figure 2a shows the volume that is associated with the specific gravity measurements using the dimensional procedure. Dimensions (height and diameter) of the sample are used to calculate the volume of the sample. Figure 2a illustrates the effect of using this volume in determining the air void content of HMA. The volume includes any surface irregularities (texture) on the outside of the sample and thus overestimates the internal air void content. Of the three cases illustrated in Figure 2, the dimensional volume is the highest, resulting in the lowest measured density.

Figure 2b illustrates the dry volume of compacted HMA samples. This volume is identical to the one derived from Equation 7 above. Because Equation 7 utilizes the dry mass in the volume determination (denominator of Equation 7), the calculated volume

does not include any of the surface irregularities on the sample or any internal air voids that are interconnected to the surface. Water that infiltrates the surface irregularities or internal voids interconnected to the surface are not considered a portion of the sample volume and, thus, provides the smallest volume of the three cases shown in Figure 2. Therefore, the dry volume underestimates the sample's true internal voids by excluding any voids interconnected to the surface. Figure 2b shows that this problem is more prevalent with mixes having coarser gradations, as there are potentially more voids interconnected to the surface of the sample.

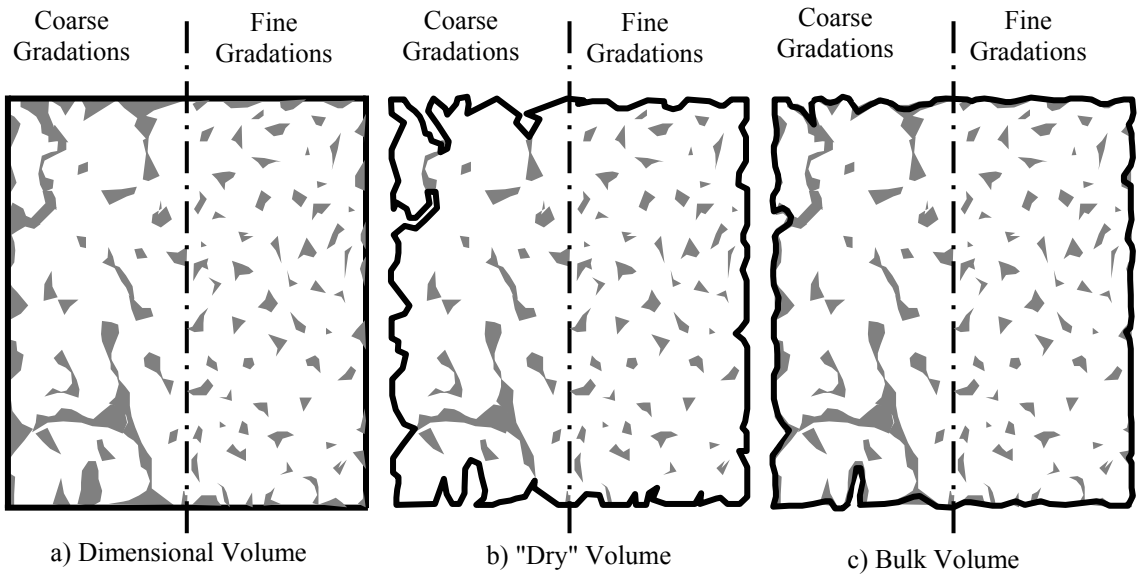

Figure 2. Volumes Associated with Compacted HMA

Figure 2c illustrates the bulk volume determined from the AASHTO T166 method. The difference between the bulk and dry volumes is that the bulk volume includes internal voids that are interconnected to the surface. This is accomplished by using the saturated-surface dry mass in the volume determination (replace M_M in the denominator of Equation 7 with the saturated-surface dry mass). The net result of using the saturated-surface dry mass is that the voids that are interconnected to the surface and

do not lose their water within the saturated-surface dry condition are included as internal voids. Therefore, the bulk volume lies between the dimensional and dry volumes.

This exercise of deriving the equation for measuring specific gravity using Archimedes' Principle and the discussion of the different volumes associated with compacted HMA illustrates the potential deficiency of the SSD method for determining bulk specific gravity of coarse-graded mixes. If the bulk volume is the desired property, which it is for HMA, then mixes with coarser gradations have a higher potential for error, as seen in Figure 2c. If a sample is submerged in water for a given time period (per standard procedure), a certain volume of water is absorbed into the sample through voids interconnected to the surface. For the coarse gradations shown in Figure 2c, this volume of interconnected voids is higher than for the fine gradations (assuming both the coarse and fine gradation mixes have the same total volume of air voids). Upon removal of the sample from the water bath, any water draining from the large interconnected voids within the coarse gradation mix leads to a lower saturated-surface dry mass. This, in effect, decreases the volume of the sample and, thus, underestimates the air void content of the sample. This is the potential drawback of the SSD method for determining the bulk specific gravity of mixes having coarse gradations. The above discussion also suggests that when the SSD method overestimates a specimen's $G_{mb,}$ the true G_{mb} should be between the G_{mb} measured by the SSD method and the G_{mb} measured by the dimensional method.

2.0 OBJECTIVES

Because of the potential errors noted with the saturated surface-dry test method of determining the bulk specific gravity of compacted HMA, the objectives of this task were: (1) compare AASHTO T166 with other methods of measuring bulk specific gravity to determine under what conditions AASHTO T166 is accurate; (2) if conditions are identified that AASHTO T166 is not applicable, identify potential improvements to AASHTO T166 to achieve a more accurate measure of bulk specific gravity; and (3) if improvements are not successful, recommend alternate methods of measuring bulk specific gravity. Results of Task 3, Part 3 are to be applicable to both laboratory compacted samples and samples taken from the roadway (cores).

3.0 SCOPE

To accomplish the objectives, two separate sample types were evaluated: laboratory compacted and field compacted. Laboratory compacted mixtures having various aggregate types, nominal maximum aggregate sizes, gradation shapes, and air void levels were prepared. Each of the prepared samples were tested to determine bulk specific gravity by four different test methods: water displacement (AASHTO T166), vacuum-sealing, gamma ray, and dimensional. Also, on a selected number of samples, the time taken to achieve SSD condition for a given sample was altered. This testing was conducted to determine the water absorption level where the potential for errors with SSD method were minimized.

For the field compacted samples, cores obtained during the field validation portion of this study were subjected to the same four bulk specific gravity test methods.

Because cores have a different surface texture than laboratory compacted samples, it was necessary to also evaluate them. Testing conducted on core samples included laboratory permeability tests and effective air void content using the vacuum-sealing device.

4.0 RESEARCH APPROACH

The overall proposed test plan is illustrated in Figure 3. This figure shows that two separate sample types were included in the experiment. Both laboratory (Superpave gyratory compactor) and field (cores) compacted samples were included because each sample type has different surface texture properties. For both sample types, four bulk specific gravity measurements were made on all samples: water displacement (AASHTO T166), vacuum-sealing (ASTM 6752-02a), gamma ray, and dimensional analysis. The following paragraphs detail the research approach for both sample types.

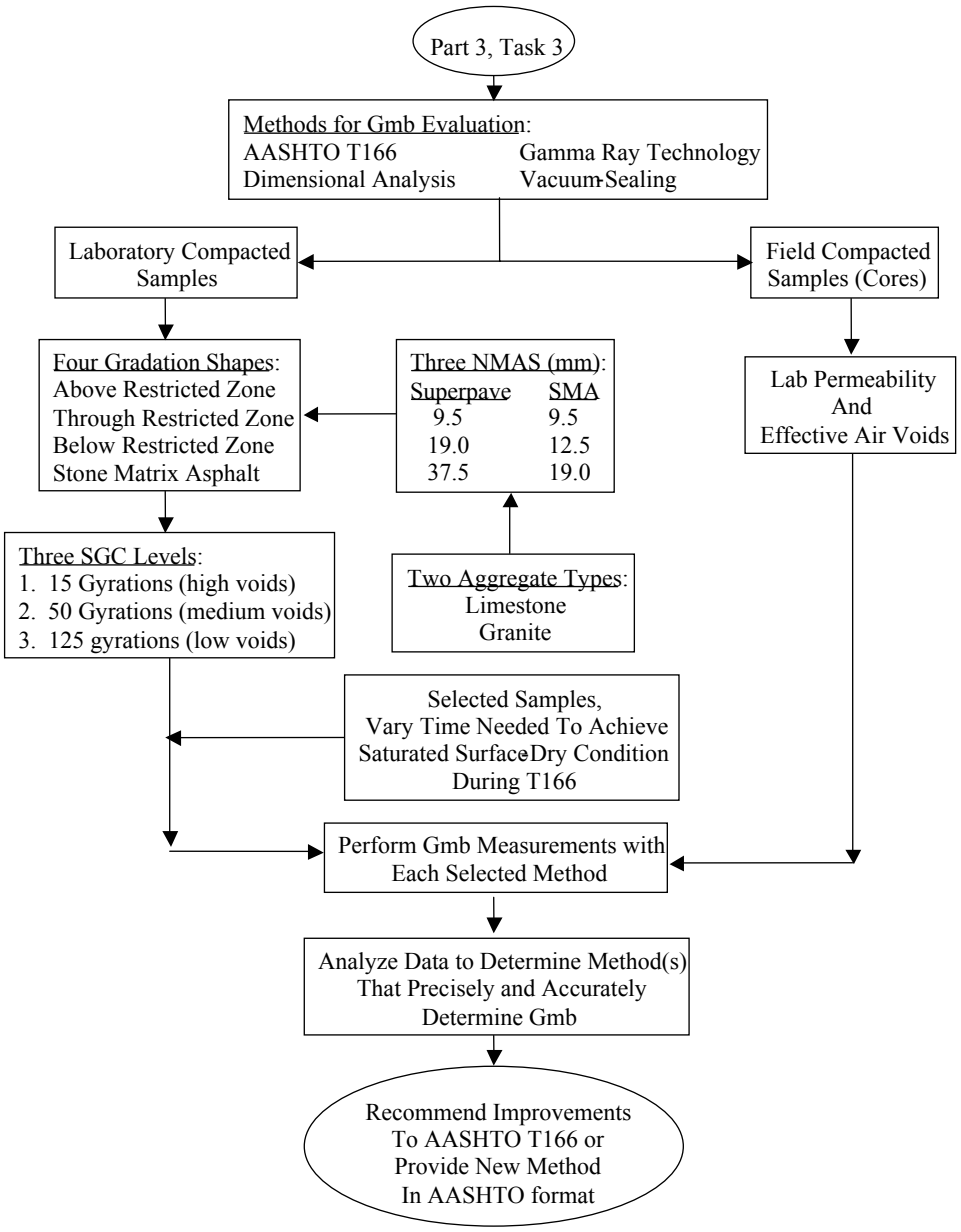

Figure 3: Research Approach for Part 3 of Task 3

4.1 Laboratory Compacted Samples

For the laboratory compacted samples, two aggregate types (limestone and granite) were used to prepare compacted samples comprised of four gradations (above, through, and below the restricted zone and SMA) at each of three nominal maximum aggregate sizes. These mixes were designed during Part 1 of Task 3 of this study. The 24

combinations of aggregate type/gradation shape/NMAS were selected because they should provide different water absorption characteristics during AASHTO T166 testing and different surface textures. Similar to Part 1, NMASs of 9.5, 19.0, and 37.5 mm were used for the Superpave designed mixes and NMASs of 9.5, 12.5, and 19.0 mm were used for the SMA mixes. At optimum asphalt content, samples were prepared using the Superpave gyratory compactor to 15, 50, and 125 gyrations to produce low, medium, and high air void contents (ranging from below 4 to approximately 12 percent) for all the mix types. Triplicate samples were prepared for each combination. To try and minimize variability in the production of these samples, a single person batched and fabricated all samples. Also, a single operator conducted all tests (bulk specific gravity measures). A single operator was used so that variability would be reduced and to allow for comparison of within-laboratory test method variabilities for the different methods utilized. This resulted in a total of 216 samples for the experiment on laboratory compacted samples.

A key component of the AASHTO T166 standard method is that the procedure is only applicable for compacted HMA having less than 2 percent water absorption by volume. As discussed previously, AASHTO T166 was originally intended for use on conventionally designed mixes (i.e., fine-graded). Therefore, a side experiment for the laboratory compacted samples was to evaluate the effect of time on water absorption, and thus G_{mb}. For this side experiment, 40 samples having a range of water absorptions (by volume) were selected from the 216 total samples. The selection of samples for various gradation shapes, NMAS, and gyration levels were also included in the experiment. Steps included in testing each sample within this side experiment included:

1. Obtain dry mass of sample.

2. Submerge sample in water bath for 10 minutes to ensure saturation of internal air voids interconnected to the surface of the sample.
3. Remove sample from water bath and let stand for two minutes.
4. Submerge sample in water bath for 4±1 minutes as per the AASHTO T166 protocol.
5. Remove sample from water bath and obtain SSD mass as fast as possible. Record SSD mass and time needed to obtain SSD condition (this occurred in six seconds).
6. Submerge sample in water bath again for 4±1 minutes as per the AASHTO T166 protocol.
7. Remove sample from water bath and obtain SSD mass after 10 seconds. Record SSD mass.
8. Follow steps 6 and 7 to obtain SSD masses after 15, 20, 30, and 60 seconds.

This testing was conducted to evaluate the sensitivity of testing time on the measured water absorption. Samples having a large proportion of interconnected voids to the surface of the sample should show decreasing water absorptions as time to achieve SSD increases. This also would correspond to an increased G_{mb}. Results of this side experiment would provide a water absorption value that leads to increased potential for errors during AASHTO T166 testing.

Analysis was conducted on the overall data set (216 samples) to determine which method(s) provided the most precise and accurate measure of the bulk specific gravity for compacted samples, regardless of the nominal maximum size, aggregate type, and air void level. If needed, changes to the current AASHTO T166 will be recommended.

4.2 Field Compacted Samples

Each of the cores obtained during the Task 5 field validation were tested to determine bulk specific gravity using the same four tests as the laboratory experiment: water displacement (AASHTO T166), vacuum sealing, gamma ray, and dimensional analysis. Because of the differences in surface texture between laboratory compacted samples (surface texture around entire sample) and field compacted samples (surface texture only on top of sample because of core bit and sawing), the experiment was also extended to core samples.

5.0 TEST METHODS AND MATERIALS

This section describes the different test methods and materials used in Task 3. The test methods included determining the bulk specific gravity of samples using water displacement (AASHTO T166), vacuum sealing, gamma ray, and dimensional analysis. Materials included some mixes designed during Part 1 of Task 3 and the cores obtained during the field validation of Task 5.

5.1 Test Methods

5.1.1 Saturated Surface-Dry Method (AASHTO T166)

The saturated surface-dry method consists of first weighing a dry sample in air, then obtaining a submerged mass after the sample has been placed in a water bath for a specified time interval (4±1 minutes). Upon removal from the water bath, the SSD mass is determined after patting the sample dry using a damp towel. Procedures for this test method are outlined in AASHTO T166 and ASTM D2726.

5.1.2 Vacuum-Sealing Test Method

Buchanan (*1*) recently reported on a comparison between the vacuum-sealing device and other more conventional G_{mb} methods that included: SSD, parafilm, and dimensional methods. This comparison indicated that the vacuum-sealing method appeared to be able to determine G_{mb} with greater accuracy than the conventional methods when samples were at low densities (i.e., high air voids). This vacuum-sealing device utilizes an automatic vacuum chamber (shown in Figure 4a) with a specially designed plastic bag, which tightly conforms to the sides of the sample (shown in Figure 4b) and prevents water from infiltrating into the sample.

Figure 4a. Vacuum-Sealing Device **Figure 4b. Sealed Sample**

The steps involved in sealing and analyzing compacted HMA samples are as follows (*2*):

Step 1: Determine the density of the plastic bag (generally provided by the manufacturer).

Step 2: Place the compacted HMA sample into the bag.

Step 3: Place the bag containing the HMA sample inside the vacuum chamber.

Step 4: Close the vacuum chamber door. The vacuum pump starts automatically and evacuates the chamber.

Step 5: In approximately two minutes, the chamber door will automatically open with the sample completely sealed within the plastic bag and ready for water displacement testing.

Step 6: Perform SSD method without obtaining SSD mass. Correct the results for the bag density and the displaced bag volume.

In addition to Buchanan (*1*), Hall *et al* (*3*) and Cooley *et al* (*4*) have also indicated that the vacuum-sealing method is a viable option for determining the G_{mb} of compacted HMA. Hall *et al* indicated that the within-lab (operator) variability for the vacuum-sealing method was less than the SSD method. Based on two separate round-robin studies, Cooley *et al* (*5*) and Spellerberg *et al* (*6*) both suggested that the vacuum-sealing method was slightly more variable (both within- and between-laboratory) than AASHTO T166; however, both round-robin studies noted that a portion of the participating laboratories had little experience with the equipment and test procedure. A standard ASTM test method has been developed for the vacuum-sealing test method, ASTM 6752-02a, "Bulk Specific Gravity and Density of Compacted Bituminous Mixtures Using Automatic Vacuum Sealing Method."

5.1.3 Gamma Ray Method

A relatively new method of determining the bulk specific gravity of HMA includes the use of gamma ray technology. This method is based upon the scattering and absorption characteristics of gamma rays within a material. The instrument works in transmission mode which means that a sample is placed between the source of gamma rays and the gamma ray detector. During the test, the device counts the gamma rays that travel through the sample in order to determine the sample's volume. Figure 5 illustrates the device used in this study.

Figure 5: Equipment for Gamma Ray Test

The steps involved in determining the bulk specific gravity of HMA samples using the gamma ray method include (*7*):

1. Using calibrated vernier calipers, measure the height of the specimen (in millimeters) in six locations and determine the average height.
2. Place the sample on the sample tray, return the tray to its home position and close the door.

3. Initiate the program.
4. Input the average sample height determined in step 1.
5. The equipment uses a four-minute count and then displays the measured bulk specific gravity.
6. Remove sample from the device.

Malpass and Khosla (*8*) reported on testing conducted at North Carolina State University to evaluate the gamma ray method for measuring the bulk specific gravity of HMA. Based upon their work, it was shown that the gamma ray and AASHTO T166 methods provided practically similar bulk specific gravity values at low to medium air void contents. However, at high air void contents, the gamma ray method provided lower values of bulk specific gravity.

5.1.4 Dimensional Method

The dimensional method of determining the bulk specific gravity included height and diameter measurements for each sample to calculate the volume of samples. The dry mass of a sample was divided by the calculated sample volume to estimate the bulk specific gravity of the sample.

5.2 Materials

As stated previously, 24 mixes from Task 3, Part 1 were included within this experiment. Also, results from the 20 field projects visited as part of Task 5 were included within this analysis. The following sections provide information on the materials used/encountered.

5.2.1 Task 3, Part 1 Laboratory Prepared Materials

Properties of the coarse and fine aggregates from Part 1 are shown in Table 1. The aggregates were selected because they represented a range of physical properties, such as absorption (0.3 to 0.9 percent), Los Angeles Abrasion (31 to 37 percent), and fine aggregate angularity (44.6 to 48.2 percent), and should provide some variability of mix properties.

Table 2 presents the test results for the asphalt cement utilized in the study. The binder was graded as PG 64-22 (meeting high temperature requirements above 67C) and is commonly used for warm climates.

Table 1: Physical Properties of Aggregate

Property		Test Method	Aggregate Type	
			Granite	Limestone
Coarse Aggregate				
Bulk Specific Gravity		AASHTO T-85	2.654	2.725
Apparent Specific Gravity		AASHTO T-85	2.704	2.758
Absorption (%)		AASHTO T-85	0.7	0.4
Flat and Elongated (%), 3:1, 5:1	19.0 mm	ASTM D4791	14, 0	10, 0
	12.5 mm		16, 0	6, 0
	9.0 mm		9, 1	16, 3
Los Angeles Abrasion (%)		AASHTO T-96	37	35
Percent Crushed (%)			100	100
Fine Aggregate				
Bulk Specific Gravity		AASHTO T-84	2.678	2.689
Apparent Specific Gravity		AASHTO T-84	2.700	2.752
Absorption (%)		AASHTO T-84	0.3	0.9
Fine Aggregate Angularity (%)		AASHTO T-33 (Method A)	45.8	44.6
Sand Equivalency (%)		AASHTO T-176	92	93

Table 2 Asphalt Binder Properties

Original		RTFOT	RTFOT+ PAV residue					
Dynamic Shear 10 rad/s		Dyn. Shear 10 rad/s	Dynamic Shear 10 rad/s		Flexural Creep (at 60 sec)			DT 1mm/min
Temp (^{o}C)	G*/sin d (kPa) 1.0 kPa min.	G*/sin d (kPa) 1.0 kPa min.	Temp. (^{o}C)	G*/sin d (kPa) 5000 kPa max.	Temp. (^{o}C)	Stiffness, S 300 Mpa max	Slope, m 0.30 min.	Strain 1.0% min
67	1.078	2.279	25	4752	-12	226	0.325	NA

NA-Results not available

Part 1 included four gradation shapes and three nominal maximum aggregate sizes (NMAS). Three gradation shapes fell within Superpave gradation control points and one gradation conformed to SMA specifications. The general mix gradations used are illustrated in Figures 6 through 9.

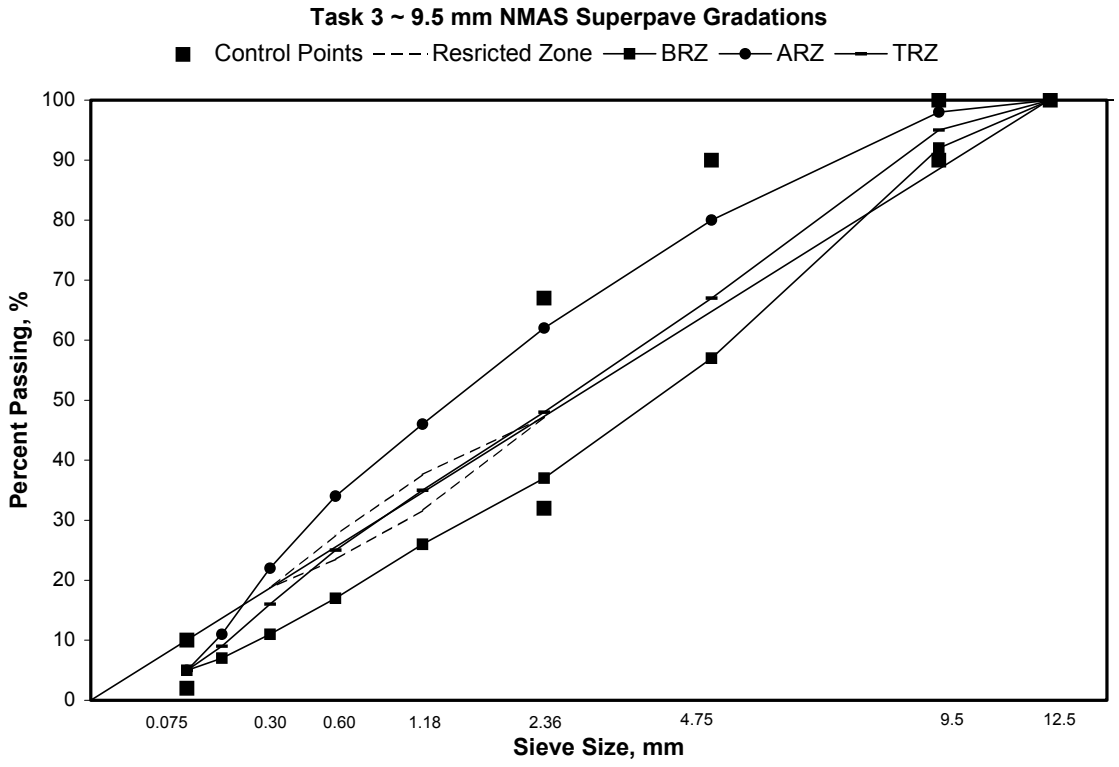

Figure 6: 9.5 mm NMAS Superpave gradations

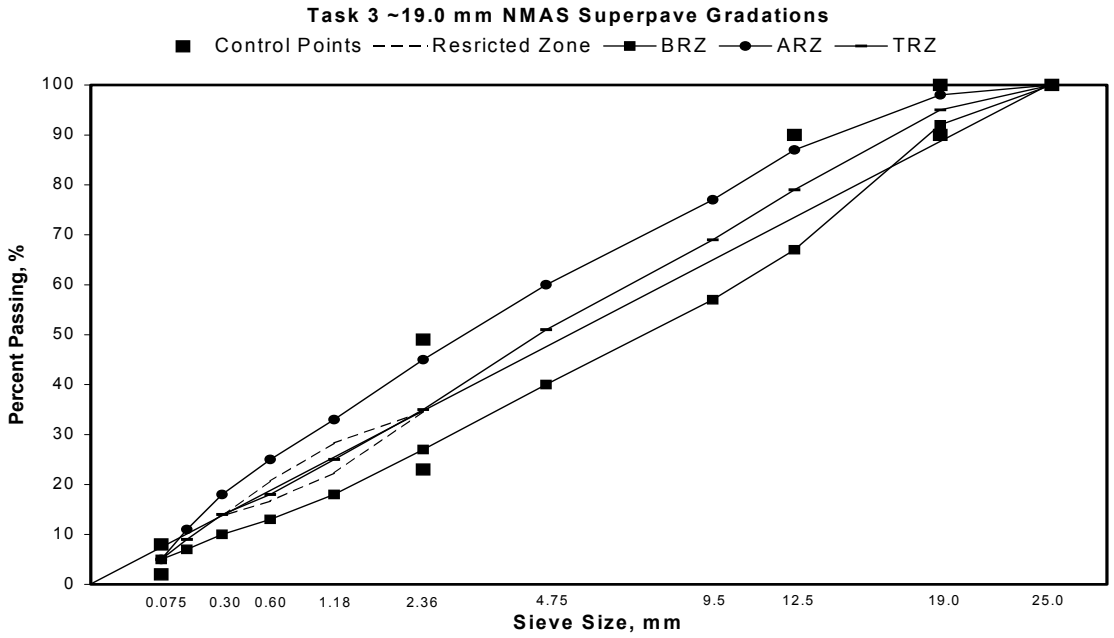

Figure 7: 19.0 mm NMAS Superpave gradations

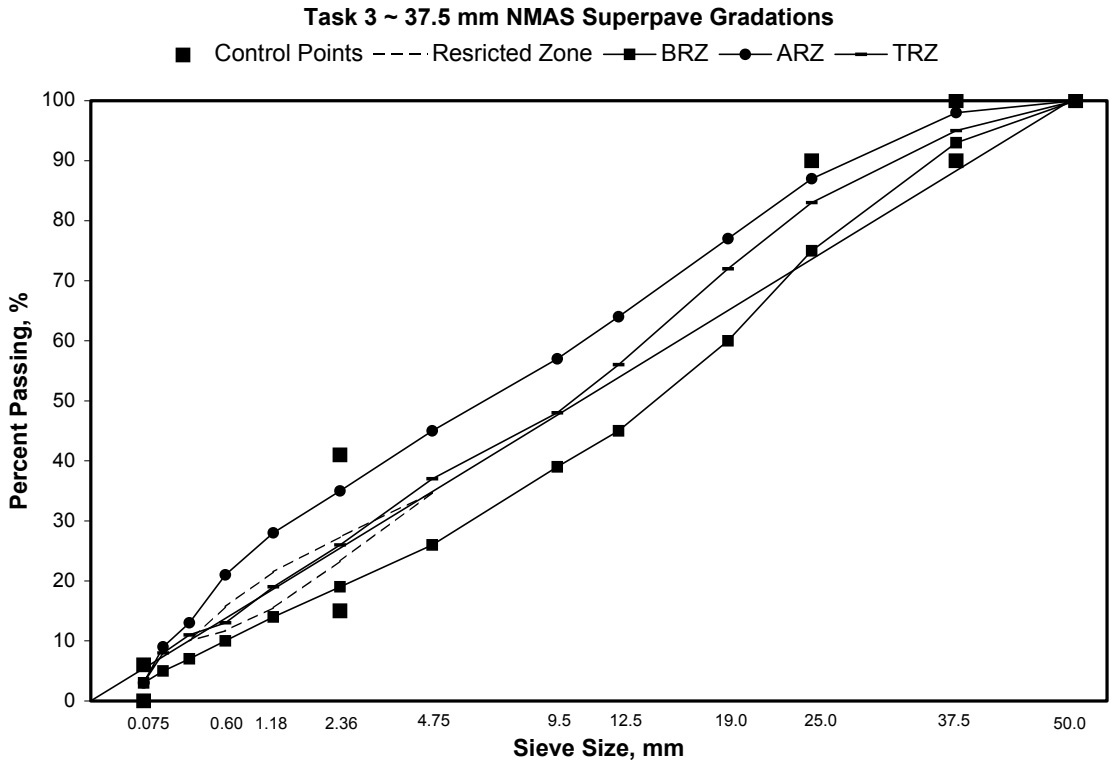

Figure 8: 37.5 mm NMAS Superpave gradations

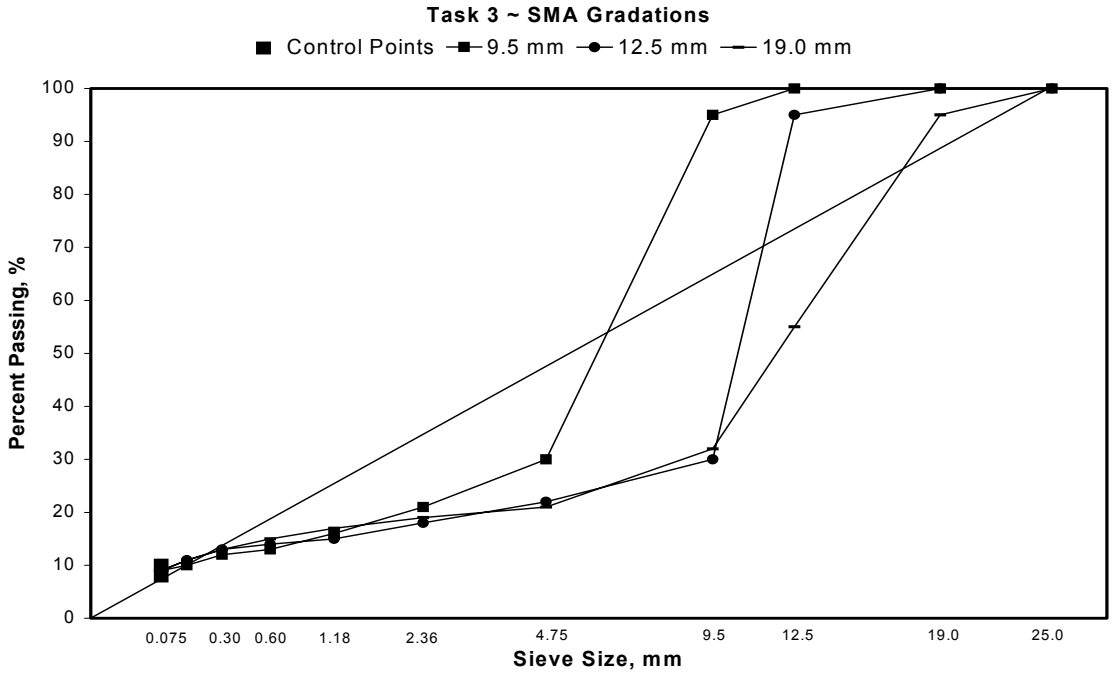

Figure 9: SMA gradations

Of the 24 mix designs utilized in this experiment, 18 were Superpave mixes and 6 were SMA mixes. For the Superpave mixes, each sample was designed to 100 gyrations in the Superpave gyratory compactor (SGC). The 100-gyration level was selected because it covers the widest range of traffic categories in the N_{design} chart within the AASHTO PP28-01, "Standard Practice for Superpave Volumetric Design for Hot–Mix Asphalt (HMA)." For the SMA mixes, each sample was designed at 75 gyrations in the SGC based on "Standard Practice for Designing SMA", AASHTO PP 44-01. The reason for using 75 gyrations was that both aggregate types had Los Angeles Abrasion values above 30 percent. Designs for both mix types were conducted to determine the asphalt binder content necessary to produce 4.0 percent air voids at the design number of gyrations. A summary of the mix designs for the Superpave and SMA mixes is presented in Table 3 and 4, respectively.

Table 3: Summary of Mix Design Information for Superpave Mixes

Agg.	NMAS	Gradation	Opt. Binder Content, %	Eff. Binder Content, %	VMA	VFA	% Gmm @N_{ini}	D/AC
Granite	9.5	ARZ	6.7	6.2	18.4	76	89.0	0.80
	9.5	BRZ	5.3	4.9	15.7	72	86.7	1.02
	9.5	TRZ	5.4	5.0	15.6	75	88.9	1.00
	19	ARZ	4.7	4.3	14.1	72	89.5	1.17
	19	BRZ	4.4	3.9	13.3	68	86.0	1.00
	19	TRZ	4.0	3.6	12.5	68	88.8	1.40
	37.5	ARZ	4.2	4.0	13.7	69	89.8	0.75
	37.5	BRZ	3.3	3.0	11.3	64	86.8	1.00
	37.5	TRZ	3.6	3.3	12.0	65	88.1	0.90
Limestone	9.5	ARZ	6.0	5.7	17.4	76	87.8	0.70
	9.5	BRZ	5.0	4.6	15.3	72	85.5	0.86
	9.5	TRZ	4.4	4.2	14.4	70	86.0	1.18
	19	ARZ	4.1	3.5	12.6	66	88.3	1.42
	19	BRZ	4.7	4.4	14.3	71	85.5	0.68
	19	TRZ	3.3	2.8	11.0	62	85.7	1.80
	37.5	ARZ	3.2	3.1	11.8	64	88.8	0.95
	37.5	BRZ	2.7	2.6	10.6	60	86.0	1.15
	37.5	TRZ	2.8	2.6	10.6	61	87.7	1.12

Table 4: Summary of Mix Design Information for SMA Mixes

Agg.	NMAS	Gradation	Opt. Binder Content, %	Eff. Binder Content, %	VMA	VFA	VCA_{mix}	VCA_{drc}
Granite	9.5	SMA	7.2	6.56	18.7	78	30.9	41.9
	12.5	SMA	6.6	6.42	18.8	77	30.3	42.7
	19	SMA	6.4	5.91	17.6	77	29.6	42.0
Limestone	9.5	SMA	6.2	5.76	17.4	76	30.7	38.4
	12.5	SMA	7.4	6.97	19.6	80	31.1	38.9
	19	SMA	6.0	5.59	16.8	77	29.8	40.3

5.2.2 Task 5 Field Projects

A total of 20 field projects were visited as part of the Task 5 field validation study. Table 5 provides information on each of the 20 projects. This table shows that six of the projects had a design NMAS of 9.5 mm. Four of these 9.5 mm NMAS mixes had fine gradations and the other two were coarse-graded. Six projects were designed as 12.5 mm NMAS gradations. Three of these six projects utilized coarse-graded gradation, two

were fine-graded, and the sixth project utilized a SMA gradation. A total of six projects were designed to have 19.0 mm NMAS gradations. Four of the six projects utilized coarse gradations, while there was one fine-graded mix and one SMA. The remaining two projects were designed to have 25.0 mm NMAS gradations, both of which were coarse-graded.

Table 5: Summary Information on Field Projects From Task 5

Project ID	NMAS	Fine or Coarse Gradation	Average Lift Thickness (mm)	Lift Thickness/ NMAS Ratio	AC Performance Grade	Ndesign
1	9.5	Fine	38.1	4:1	70-22	65
2	19.0	Coarse	63.5	4:1	64-22	65
3	9.5	Coarse	38.1	4:1	64-22	65
4	9.5	Fine	68.6	5:1	NA	75
5	9.5	Fine	31.8	3:1	70-22	100
6	12.5	Coarse	57.2	4:1	58-28	75
7	12.5	Fine	50.8	4:1	64-28	75
8	19.0	Coarse	50.8	3:1	64-22	100
9	25.0	Coarse	101.6	4:1	64-22	100
10	19.0	Coarse	57.2	3:1	64-34	100
11	19.0	Coarse	38.1	2:1	64-34	125
12	19.0	SMA	61.0	3:1	76-22	50
13	25.0	Coarse	70.0	3:1	67-22	100
14	12.5	SMA	26.8	3:1	76-22	75
15	19.0	Fine	50.4	3:1	76-22	100
16	9.5	Fine	43.8	4:1	67-22	86
17	12.5	Fine	50.8	3:1	64-22	75
18	12.5	Coarse	38.1	3:1	67-22	75
19	9.5	Coarse	31.8	3:1	67-22	75
20	12.5	Coarse	38.1	3:1	67-22	80

6.0 TEST RESULTS AND ANALYSIS

Within this section, test results and analyses are provided for the experiments to recommend improvements to AASHTO T166. Because of the potential differences in conclusions between laboratory and field compacted samples, this section is divided into two primary subsections that describe test results and analyses for each sample type.

6.1 Laboratory Compacted Samples

Results of bulk specific gravity measurements on the 24 laboratory mixes at the three gyration levels are presented in Tables 6 through 13. These tables include results of bulk specific gravity measurements using the four test methods: water displacement, vacuum sealing, gamma ray, and dimensional analysis.

Table 6: Results of Part 3 Testing for 9.5 mm NMAS Limestone Mixes

			Bulk Specific Gravity, Gmb			
Gradation	Gyration	Replicate	Dimensional	Gamma Ray	Vacuum-Seal	AASHTO T166
ARZ	15	1	2.238	2.227	2.268	2.267
	15	2	2.234	2.226	2.265	2.266
	15	3	2.235	2.232	2.259	2.263
	50	1	2.329	2.341	2.354	2.356
	50	2	2.333	2.333	2.348	2.354
	50	3	2.332	2.333	2.371	2.357
	125	1	2.390	2.390	2.405	2.411
	125	2	2.391	2.393	2.408	2.413
	125	3	2.383	2.392	2.409	2.407
BRZ	15	1	2.168	2.189	2.217	2.245
	15	2	2.166	2.192	2.212	2.254
	15	3	2.188	2.204	2.227	2.255
	50	1	2.306	2.334	2.343	2.362
	50	2	2.311	2.344	2.336	2.356
	50	3	2.298	2.354	2.343	2.363
	125	1	2.383	2.417	2.420	2.431
	125	2	2.391	2.422	2.430	2.443
	125	3	2.389	2.423	2.421	2.429
TRZ	15	1	2.225	2.258	2.267	2.292
	15	2	2.240	2.280	2.270	2.296
	15	3	2.242	2.269	2.279	2.300
	50	1	2.369	2.402	2.405	2.416
	50	2	2.362	2.400	2.405	2.414
	50	3	2.367	2.397	2.396	2.409
	125	1	2.440	2.461	2.465	2.469
	125	2	2.434	2.463	2.465	2.470
	125	3	2.445	2.472	2.466	2.473

Table 7: Results of Part 3 Testing for 9.5 mm NMAS Granite Mixes

			Bulk Specific Gravity, Gmb			
Gradation	Gyration	Replicate	Dimensional	Gamma Ray	Vacuum Seal	AASHTO T166
ARZ	15	1	2.192	2.181	2.221	2.224
	15	2	2.189	2.205	2.218	2.218
	15	3	2.192	2.180	2.226	2.222
	50	1	2.271	2.281	2.303	2.302
	50	2	2.268	2.273	2.304	2.300
	50	3	2.280	2.279	2.299	2.297
	125	1	2.316	2.327	2.345	2.340
	125	2	2.315	2.328	2.338	2.345
	125	3	2.323	2.326	2.351	2.348
BRZ	15	1	2.157	2.166	2.198	2.231
	15	2	2.169	2.206	2.210	2.236
	15	3	2.158	2.208	2.200	2.229
	50	1	2.258	2.286	2.302	2.318
	50	2	2.269	2.305	2.304	2.322
	50	3	2.293	2.318	2.309	2.322
	125	1	2.348	2.381	2.355	2.393
	125	2	2.342	2.367	2.381	2.390
	125	3	2.350	2.365	2.389	2.396
TRZ	15	1	2.207	2.206	2.241	2.255
	15	2	2.212	2.206	2.247	2.255
	15	3	2.199	2.226	2.235	2.249
	50	1	2.302	2.313	2.322	2.330
	50	2	2.283	2.301	2.316	2.324
	50	3	2.284	2.300	2.324	2.329
	125	1	2.342	2.359	2.374	2.375
	125	2	2.337	2.361	2.366	2.371
	125	3	2.348	2.370	2.375	2.379

Table 8: Results of Part 3 Testing for 19.0mm NMAS Limestone Mixes

			Bulk Specific Gravity, Gmb			
Gradation	Gyration	Replicate	Dimensional	Gamma Ray	Vacuum-Seal	AASHTO T166
ARZ	15	1	2.299	2.326	2.335	2.346
	15	2	2.296	2.314	2.335	2.345
	15	3	2.291	2.306	2.329	2.331
	50	1	2.377	2.400	2.413	2.418
	50	2	2.369	2.394	2.405	2.410
	50	3	2.370	2.407	2.409	2.414
	125	1	2.449	2.475	2.480	2.480
	125	2	2.452	2.490	2.475	2.476
	125	3	2.461	2.481	2.483	2.483
BRZ	15	1	2.187	2.211	2.247	2.297
	15	2	2.191	2.203	2.223	2.289
	15	3	2.188	2.221	2.229	2.304
	50	1	2.319	2.358	2.368	2.393
	50	2	2.332	2.375	2.380	2.409
	50	3	2.331	2.382	2.382	2.413
	125	1	2.412	2.456	2.449	2.474
	125	2	2.403	2.440	2.447	2.472
	125	3	2.432	2.449	2.457	2.469
TRZ	15	1	2.273	2.391	2.317	2.351
	15	2	2.270	2.372	2.321	2.362
	15	3	2.267	2.354	2.322	2.363
	50	1	2.373	2.423	2.424	2.449
	50	2	2.373	2.439	2.423	2.456
	50	3	2.367	2.430	2.418	2.453
	125	1	2.457	2.507	2.497	2.517
	125	2	2.463	2.514	2.504	2.516
	125	3	2.490	2.526	2.514	2.522

Table 9: Results of Part 3 Testing on 19.0 mm NMAS Granite Mixes

			Bulk Specific Gravity, Gmb			
Gradation	Gyration	Replicate	Dimensional	Gamma Ray	Vacuum-Seal	AASHTO T166
ARZ	15	1	2.230	2.263	2.280	2.298
	15	2	2.252	2.275	2.289	2.304
	15	3	2.252	2.257	2.285	2.300
	50	1	2.330	2.338	2.367	2.370
	50	2	2.308	2.336	2.357	2.368
	50	3	2.321	2.346	2.332	2.366
	125	1	2.370	2.396	2.407	2.410
	125	2	2.384	2.399	2.397	2.410
	125	3	2.364	2.383	2.378	2.407
BRZ	15	1	2.167	2.223	2.244	2.302
	15	2	2.179	2.223	2.236	2.322
	15	3	2.191	2.251	2.243	2.320
	50	1	2.296	2.372	2.356	2.397
	50	2	2.290	2.349	2.352	2.388
	50	3	2.298	2.357	2.356	2.388
	125	1	2.360	2.444	2.415	2.442
	125	2	2.362	2.404	2.418	2.441
	125	3	2.368	2.415	2.431	2.456
TRZ	15	1	2.211	2.269	2.285	2.311
	15	2	2.230	2.250	2.279	2.283
	15	3	2.222	2.297	2.274	2.298
	50	1	2.328	2.357	2.381	2.395
	50	2	2.332	2.359	2.374	2.389
	50	3	2.341	2.366	2.374	2.392
	125	1	2.379	2.427	2.415	2.421
	125	2	2.384	2.419	2.420	2.426
	125	3	2.365	2.408	2.414	2.425

Table 10: Results of Part 3 Testing for Limestone SMA Mixes

			Bulk Specific Gravity, Gmb			
NMAS	Gyration	Replicate	Dimensional	Gamma Ray	Vacuum-Seal	AASHTO T166
9.5 mm	15	1	2.123	2.169	2.183	2.251
	15	2	2.124	2.194	2.186	2.251
	15	3	2.127	2.176	2.166	2.244
	50	1	2.281	2.351	2.330	2.355
	50	2	2.263	2.329	2.314	2.342
	50	3	2.266	2.307	2.333	2.359
	125	1	2.418	2.458	2.444	2.466
	125	2	2.412	2.464	2.437	2.465
	125	3	2.404	2.433	2.429	2.456
12.5 mm	15	1	2.105	2.160	2.179	2.237
	15	2	2.113	2.129	2.163	2.232
	15	3	2.105	2.119	2.181	2.244
	50	1	2.231	2.288	2.291	2.320
	50	2	2.223	2.303	2.278	2.320
	50	3	2.235	2.312	2.306	2.331
	125	1	2.303	2.349	2.363	2.389
	125	2	2.327	2.381	2.368	2.393
	125	3	2.317	2.358	2.380	2.398
19.0 mm	15	1	2.066	2.096	2.162	2.306
	15	2	2.069	2.093	2.172	2.296
	15	3	2.050	2.143	2.159	2.293
	50	1	2.260	2.382	2.323	2.382
	50	2	2.255	2.382	2.343	2.388
	50	3	2.291	2.364	2.376	2.405
	125	1	2.384	2.474	2.430	2.457
	125	2	2.359	2.501	2.421	2.450
	125	3	2.368	2.491	2.432	2.447

Table 11: Results of Part 3 Testing for Granite SMA Mixes

			Bulk Specific Gravity, Gmb			
NMAS	Gyration	Replicate	Dimensional	Gamma Ray	Vacuum-Seal	AASHTO T166
9.5 mm	15	1	2.036	2.119	2.109	2.207
	15	2	2.045	2.126	2.115	2.192
	15	3	2.055	2.160	2.119	2.191
	50	1	2.192	2.313	2.258	2.277
	50	2	2.209	2.323	2.268	2.296
	50	3	2.206	2.304	2.271	2.295
	125	1	2.282	2.387	2.337	2.355
	125	2	2.280	2.385	2.339	2.355
	125	3	2.284	2.378	2.337	2.357
12.5 mm	15	1	2.041	2.056	2.125	2.259
	15	2	2.016	2.045	2.097	2.224
	15	3	2.016	2.147	2.110	2.258
	50	1	2.167	2.240	2.250	2.311
	50	2	2.179	2.288	2.258	2.310
	50	3	2.180	2.309	2.266	2.287
	125	1	2.274	2.394	2.333	2.359
	125	2	2.276	2.334	2.344	2.372
	125	3	2.276	2.388	2.337	2.360
19.0 mm	15	1	2.010	2.108	2.141	2.269
	15	2	2.064	2.104	2.164	2.284
	15	3	2.003	2.106	2.102	2.262
	50	1	2.278	2.350	2.380	2.430
	50	2	2.210	2.228	2.308	2.366
	50	3	2.156	2.244	2.254	2.336
	125	1	2.289	2.360	2.369	2.400
	125	2	2.301	2.350	2.368	2.400
	125	3	2.278	2.328	2.354	2.386

Table 12: Results of Part 3 Testing on 37.5 mm NMAS Limestone Mixes

			Bulk Specific Gravity, Gmb			
Gradation	Gyration	Replicate	Dimensional	Gamma Ray	Vacuum-Seal	AASHTO T166
ARZ	15	1	2.252	2.290	2.325	2.373
	15	2	2.215	2.286	2.308	2.349
	15	3	2.299	2.353	2.313	2.381
	50	1	2.388	2.446	2.434	2.453
	50	2	2.365	2.467	2.427	2.448
	50	3	2.383	2.451	2.417	2.448
	125	1	2.418	2.471	2.460	2.493
	125	2	2.431	2.471	2.484	2.498
	125	3	2.457	2.505	2.492	2.504
BRZ	15	1	2.182	2.218	2.268	2.443
	15	2	2.192	2.234	2.265	2.442
	15	3	2.201	2.268	2.256	2.441
	50	1	2.290	2.393	2.423	2.497
	50	2	2.276	2.389	2.406	2.495
	50	3	2.311	2.390	2.390	2.456
	125	1	2.421	2.473	2.485	2.521
	125	2	2.413	2.489	2.471	2.522
	125	3	2.401	2.505	2.475	2.552
TRZ	15	1	2.193	2.285	2.296	2.366
	15	2	2.187	2.294	2.294	2.381
	15	3	2.250	2.307	2.320	2.387
	50	1	2.322	2.435	2.421	2.466
	50	2	2.364	2.439	2.427	2.462
	50	3	2.360	2.487	2.409	2.491
	125	1	2.428	2.481	2.499	2.532
	125	2	2.422	2.490	2.470	2.528
	125	3	2.422	2.493	2.488	2.523

Table 13: Results of Part 3 Testing on 37.5 mm NMAS Granite Mixes

			Bulk Specific Gravity, Gmb			
Gradation	Gyration	Replicate	Dimensional	Gamma Ray	Vacuum-Seal	AASHTO T166
ARZ	15	1	2.226	2.265	2.283	2.319
	15	2	2.224	2.282	2.269	2.304
	15	3	2.204	2.324	2.270	2.306
	50	1	2.318	2.551	2.361	2.368
	50	2	2.315	2.547	2.349	2.368
	50	3	2.338	2.585	2.356	2.379
	125	1	2.374	2.501	2.413	2.427
	125	2	2.365	2.501	2.401	2.421
	125	3	2.385	2.442	2.410	2.425
BRZ	15	1	2.066	2.109	2.219	2.390
	15	2	2.087	2.155	2.194	2.378
	15	3	2.108	2.175	2.218	2.382
	50	1	2.271	2.457	2.340	2.399
	50	2	2.228	2.360	2.338	2.424
	50	3	2.232	2.437	2.337	2.408
	125	1	2.376	2.462	2.435	2.464
	125	2	2.332	2.456	2.409	2.458
	125	3	2.330	2.459	2.421	2.464
TRZ	15	1	2.195	2.320	2.293	2.361
	15	2	2.212	2.329	2.340	2.410
	15	3	2.260	2.407	2.295	2.403
	50	1	2.292	2.436	2.361	2.392
	50	2	2.236	2.492	2.377	2.405
	50	3	2.297	2.461	2.376	2.413
	125	1	2.342	2.488	2.381	2.447
	125	2	2.349	2.484	2.404	2.448
	125	3	2.360	2.475	2.365	2.450

Bulk specific gravity values shown in Tables 6 through 13 were converted to air void contents for some analyses. This was done because each of the aggregate/gradation combinations had different bulk specific gravities for the aggregate. An initial analysis of variance (ANOVA) was conducted on the air voids data to determine whether the different methods yielded different bulk specific gravity measurements on similar mixes. If all four methods resulted in similar air void contents, then no modifications to AASHTO T166 would be required. However, if the different methods produced

significantly different air void contents then the next course of action would be to determine which method provided a better overall estimate of bulk specific gravity. If AASHTO T166 was not the most accurate method over all values of NMAS, gradation shapes and air void contents, then analyses were needed to determine when AASHTO T166 was applicable, identify potential improvements to AASHTO T166 to achieve a more accurate measure of bulk specific gravity, or recommend alternate methods of measuring bulk specific gravity.

Two separate ANOVAs were conducted: one for the Superpave mixes and one for the SMA mixes. The data was separated in this manner because combining the two data sets into a single data set would result in an unbalanced experimental design. The Superpave and SMA data sets contained different NMAS.

Results of the ANOVA conducted on the Superpave mix data are presented in Table 14. All five main factors (gradation shape, aggregate type, NMAS, gyration level, and method) significantly affected air void contents. There were also a large number of two- and three-way interactions that were significant. Based upon the F-statistics, the gyration level (compactive effort) had the greatest effect on resulting air void contents. The next most significant factor was bulk specific gravity method.

Because of the differences in resulting air voids for the four methods of measuring bulk specific gravity, a Duncan's multiple range test (DMRT) was conducted to determine which methods, if any, provided similar results. This analysis method provides a ranking comparison between the different methods. The range of sample means for a given set of data (method) can be compared to a critical valued based on the

Table 14: Results of ANOVA Conducted on Superpave Designed Mixes

Source	DF	Mean Squares	$F_{Statistic}$	$F_{Critical}$	Significant (α=0.05)?
Aggregate Type (Agg.)	1	7.45	26.21	3.84	Yes
Nominal Max. Agg. Size (NMAS)	2	39.20	137.92	3.00	Yes
Gradation Shape (Grad.)	2	132.28	465.33	3.00	Yes
Gyration Level (Gyr.)	2	2304.71	8107.76	3.00	Yes
Bulk Specific Gravity Method (Meth.)	3	282.49	993.76	2.60	Yes
Agg*NMAS	2	10.95	38.52	3.00	Yes
Agg.*Grad	2	0.89	3.15	3.00	Yes
Agg*Gyr	2	18.28	64.32	3.00	Yes
Agg*Meth	3	5.37	18.88	2.60	Yes
NMAS*Grad	4	7.92	27.86	2.37	Yes
NMAS*Gyr	4	2.22	7.81	2.37	Yes
NMAS*Meth	6	39.81	140.04	2.10	Yes
Grad*Gyr	4	21.28	74.88	2.37	Yes
Grad*Meth	6	19.13	67.31	2.10	Yes
Gyr*Meth	6	15.75	55.42	2.10	Yes
Agg*NMAS*Grad	4	11.38	40.04	2.37	Yes
Agg*NMAS*Gyr	4	1.31	4.62	2.37	Yes
Agg*NMAS*Meth	6	8.85	31.14	2.10	Yes
Agg*Grad*Gyr	4	3.66	12.89	2.37	Yes
Agg*Grad*Meth	6	0.63	2.20	2.10	Yes
Agg*Gyr*Meth	6	1.52	5.35	2.10	Yes
NMAS*Grad*Gyr	8	2.68	9.44	1.94	Yes
NMAS*Grad*Meth	12	5.80	20.39	1.75	Yes
NMAS*Gyr*Meth	12	6.02	21.16	1.75	Yes
Grad*Gyr*Meth	12	2.44	8.57	1.75	Yes
Agg*NMAS*Grad*Gyr	8	3.73	13.11	1.94	Yes
Agg*NMAS*Grad*Meth	12	1.05	3.70	1.75	Yes
Agg*NMAS*Gyr*Meth	12	1.48	5.20	1.75	Yes
Agg*Grad*Gyr*Meth	12	0.36	1.28	1.75	No
NMAS*Grad*Gyr*Meth	24	0.88	3.08	1.52	Yes
Agg*NMAS*Grad*Gyr*Meth	24	0.46	1.62	1.52	Yes
Error	432	0.28	---	---	---

percentiles of the sampling distribution. The critical value is based on the number of means being compared (four, representing the different methods) and the number of degrees of freedom at a given level of significance (0.05 for this analysis). Results of the DMRT analysis for the Superpave mixes are illustrated in Figure 10.

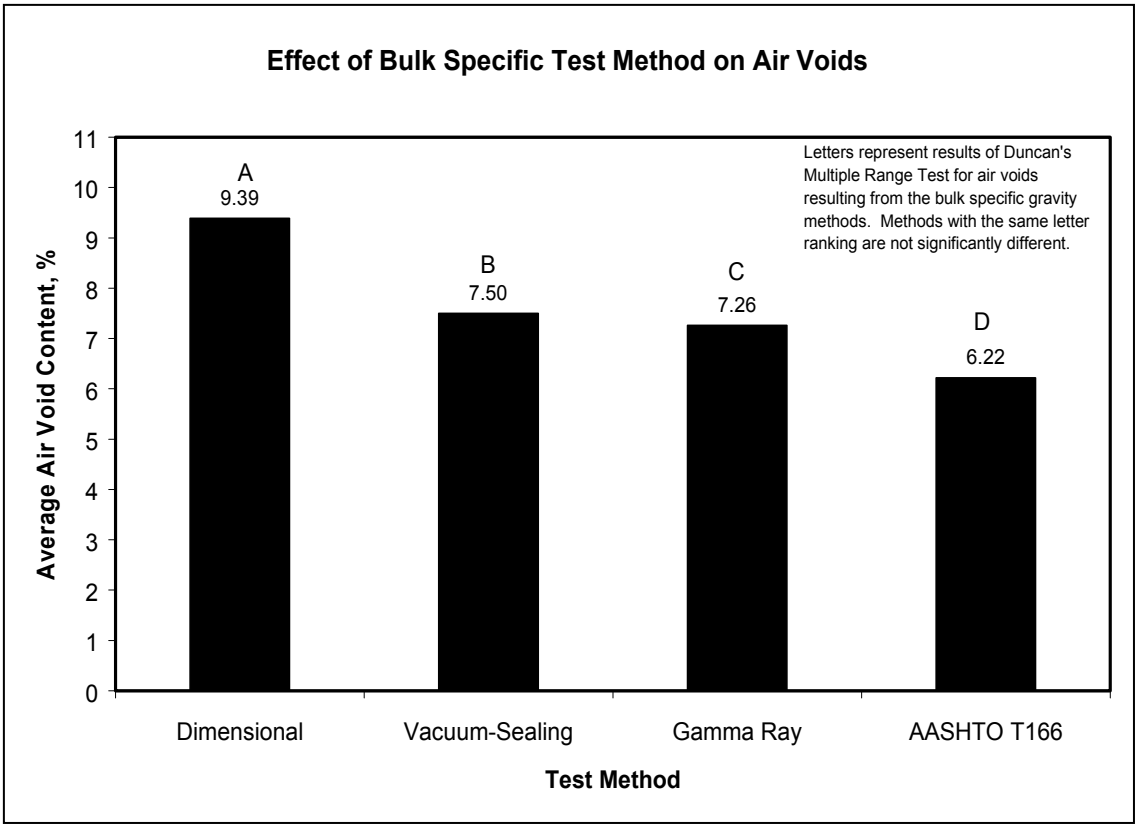

Figure 10: Average Air Voids and DMRT Results for Superpave Mixes

Statistically, results of the DMRT comparisons showed that all methods produced differing resulting air void contents. However, vacuum-sealing and gamma ray bulk specific gravity methods practically provided similar results given a difference of 0.24 percent air voids. On average, the dimensional method resulted in the highest air void contents, followed by the vacuum-sealing and gamma ray methods, respectively. Air void contents determined from AASHTO T166 were the lowest. None of the alternative methods provided similar results to AASHTO T166.

Results of the ANOVA conducted for the SMA mixes are presented in Table 15. Factors included within the ANOVA were aggregate type, NMAS, gyration level, and bulk specific gravity method. All of the main factors except NMAS significantly affected

the resulting air void contents. The factor having the most affect was gyration level followed by bulk specific gravity method and aggregate type.

Table 15: Results of ANOVA Conducted on SMA Mixes

Source	DF	Mean Squares	$F_{Statistic}$	$F_{Critical}$	Significant (α=0.05)?
Aggregate Type (Agg.)	1	17.31	25.14	3.84	Yes
Nominal Max. Agg. Size (NMAS)	2	11.63	16.89	3.00	Yes
Gyration Level (Gyr.)	2	1624.87	2359.26	3.00	Yes
Bulk Specific Gravity Meth. (Meth.)	3	240.28	348.88	2.60	Yes
Agg*NMAS	2	7.57	10.99	3.00	Yes
Agg*Gyr	2	5.44	7.90	3.00	Yes
Agg*Meth	3	3.99	5.79	2.60	Yes
NMAS*Gyr	4	6.55	9.51	2.37	Yes
NMAS*Meth	6	6.87	9.98	2.10	Yes
Gyr*Meth	6	24.50	35.57	2.10	Yes
Agg*NMAS*Gyr	4	5.08	7.38	2.37	Yes
Agg*NMAS*Meth	6	3.40	4.93	2.10	Yes
Agg*Gyr*Meth	6	0.5	0.70	2.10	No
NMAS*Gyr*Meth	12	1.20	1.74	1.75	No
Agg*NMAS*Gyr*Meth	12	1.65	2.39	1.75	Yes
Error	215	0.69	---	---	---

Because bulk specific gravity method significantly affected the resulting air voids, a DMRT analysis was again conducted to determine which methods provided similar results (if any). Results of the DMRT analysis are presented in Figure 11. Similar to the Superpave mixes, the vacuum-sealing and gamma ray methods resulted in similar air void contents. The dimensional method resulted in the highest air voids and the AASHTO T166 method resulted in the lowest air voids.

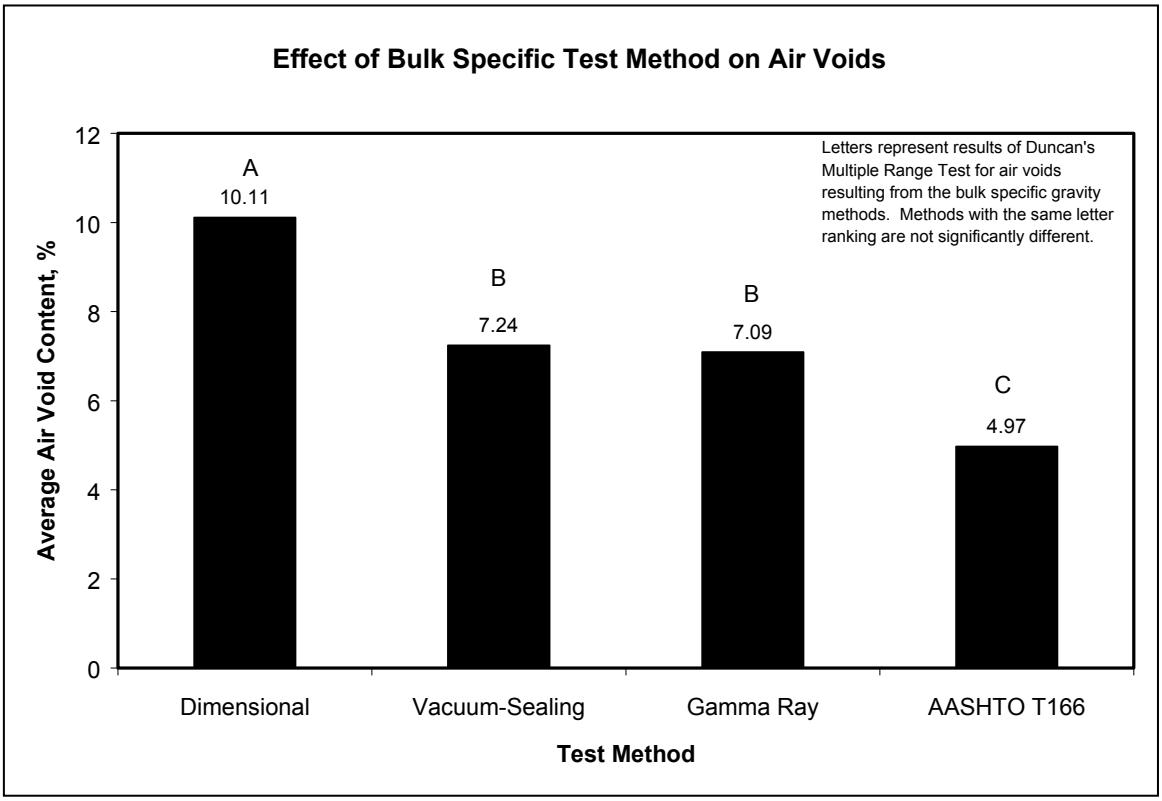

Figure 11: Average Air Voids and DMRT Results for SMA Mixes

Analysis of both the Superpave and SMA data indicated that the four methods of measuring bulk specific gravity significantly affected resulting air voids. For both mix types, the vacuum-sealing and gamma ray methods provided similar air voids; however, the dimensional method provided significantly higher air voids and AASHTO T166 provided significantly lower air void contents.

Theoretically, the dimensional method should provide the highest measured air void content as this method includes both the internal air voids and the surface texture of the sample. Therefore, the results in Figures 10 and 11 pass the test of reasonableness for the vacuum-sealing, gamma ray, and AASHTO T166 methods as all three provided air void contents less than the dimensional method.

Previously within this report, the potential problems with the AASHTO T166 method were discussed, namely the loss of water through surface connected voids during determination of saturated-surface dry (SSD) mass. When the sample loses water during determination of the SSD mass, AASHTO T166 would be expected to overestimate actual density (i.e. air voids are lower). Therefore, if the vacuum-sealing and gamma ray methods are providing good estimates of bulk specific gravity when all of the data was compared, then the results of the DMRTs for the Superpave and SMA mixes appear to be make sense as the AASHTO T166 results provided the lowest air void contents. However, this finding needs to be verified through further analyses.

The hypothesis for evaluating the vacuum-sealing, gamma ray, and AASHTO T166 bulk specific gravity methods was that the water displacement method is accurate at low levels of water absorption. This has been shown (or assumed) by numerous researchers (*1*, *4*, *9*, and *10*). Therefore, one method of determining the acceptability of the vacuum-sealing and gamma ray methods would be to compare these methods to AASHTO T166 results with samples having low water absorptions.

Based upon the experimental plan for the study, mixes having low water absorptions would include the fine-graded (ARZ) mixes compacted to 125 gyrations. To verify which mixtures had low water absorption values, the average water absorption levels per mix type (a given NMAS, gradation, and gyration level) were plotted in Figure 12. This figure illustrates that mixes meeting the ARZ gradation had the lowest water absorption level of the gradations studied. Also, samples compacted at 125 gyrations did in fact have the lowest water absorption levels. Mixes having ARZ gradations and a NMAS of 9.5 and 19.0 mm had average water absorption levels well below 0.5 percent.

Therefore, an ANOVA was conducted on the air void contents results from the 9.5 and 19.0 mm NMAS mixes having an ARZ gradation compacted to 125 gyrations. The average water absorption value for the 48 samples included in the ANOVA was 0.20 percent with a standard deviation of 0.14 percent. Factors included in the ANOVA were aggregate type, NMAS, and test method. This ANOVA was conducted to determine if the different methods of measuring bulk specific gravity provided similar results when water absorption levels are low and AASHTO T166 is accurate. Based on the ANOVA, the four methods of measuring bulk specific gravity provided significantly different air void contents. Therefore, a DMRT ranking was conducted to determine which, if any, of the methods provided similar results. Results of the DMRT are presented in Figure 13.

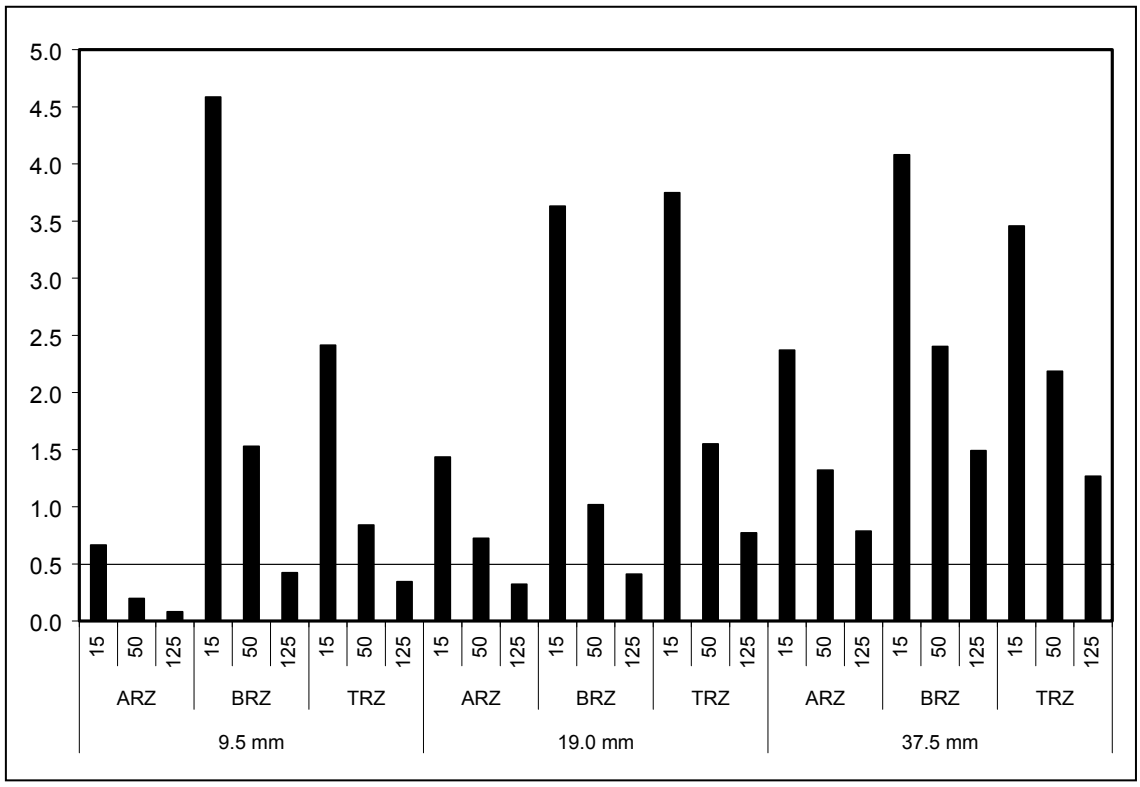

Figure 12: Water Absorption Levels by NMAS, Gradation, and Gyration Level

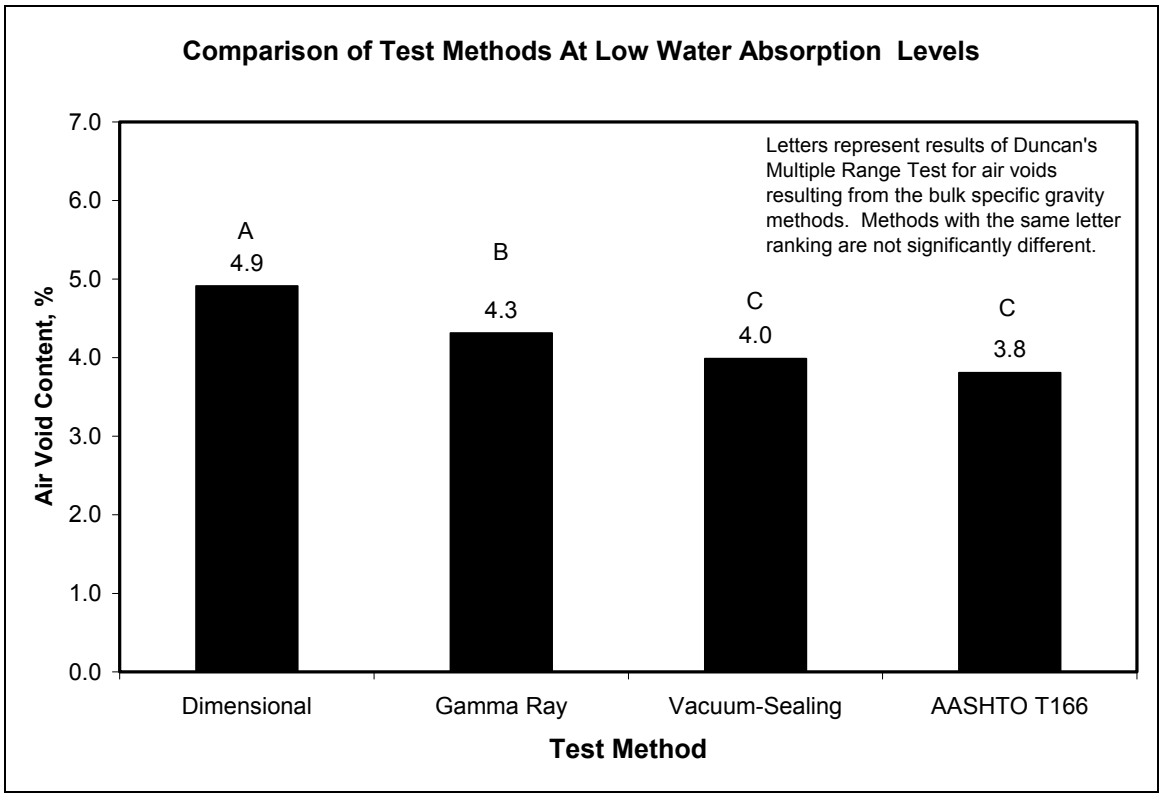

Figure 13: Comparison of Test Methods for Low Water Absorption Level Mixes

Figure 13 shows that the vacuum-sealing and AASHTO T166 methods provided similar results and both were significantly different than the dimensional and gamma ray methods. The dimensional method provided the highest air void content, as expected. If the AASHTO T166 method is accurate for low water absorption mixes, then these results suggest that the vacuum-sealing method is the only other method that is also accurate. Figures 10 and 11 suggest that the gamma ray method does an overall adequate job of estimating bulk specific gravity; however, Figure 13 suggests that it is not as accurate as AASHTO T166 or the vacuum-sealing methods. Refinements to the gamma ray method may make this method a viable option in the future.

The next step in analyzing the data was to compare test results from the vacuum-sealing and AASHTO T166 methods for all combinations of materials utilized in the

study. Figures 14 through 21 illustrate the comparisons between the vacuum-sealing and AASHTO T166 methods. The different figures reflect different aggregate types since the ANOVA conducted on the overall data set (Tables 14 and 15) indicated that aggregate type significantly affected the resulting air voids.

Figure 14 illustrates the comparison between the vacuum-sealing and AASHTO T166 methods for mixes comprised of the limestone aggregate and having a NMAS of 9.5 mm. Figure 15 presents the comparisons for the granite mixes. Four gradation shapes are illustrated on both figures: ARZ, BRZ, TRZ, and SMA. Paired *t*-tests were conducted to determine whether there were differences between the two methods for each of the mix types (gradation-gyration level).

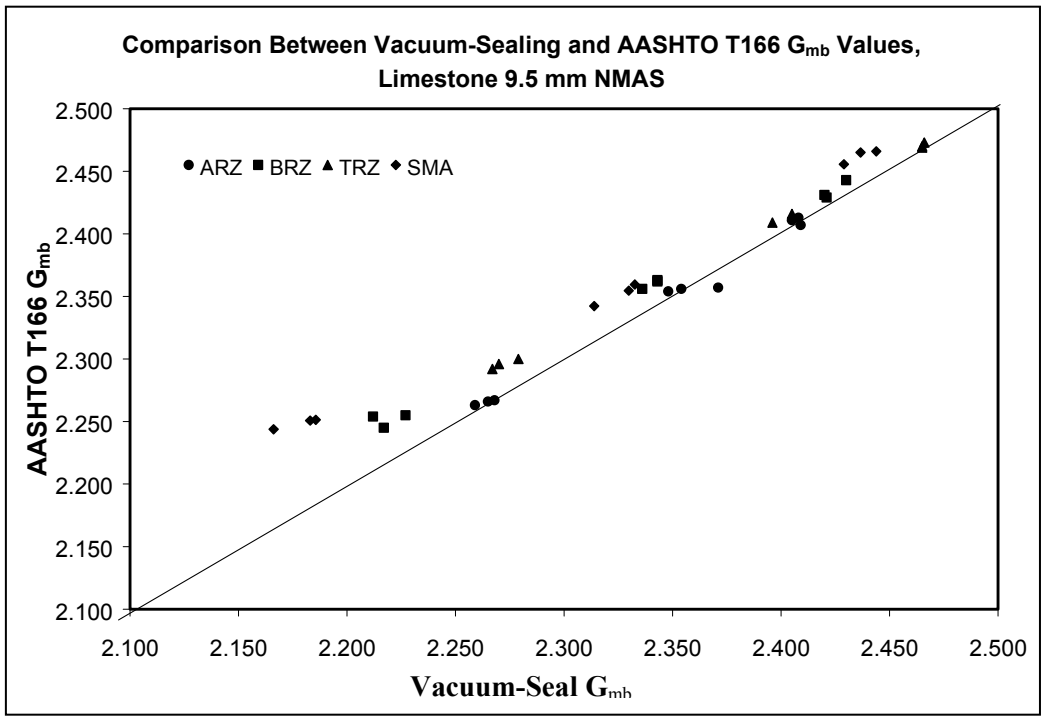

Figure 14: Comparison Between Vacuum-Sealing and AASHTO T166 Methods, 9.5 mm Limestone

Actual bulk specific gravity values were used in this analysis. No matter the gyration level, the two methods yielded similar results for the fine-graded (ARZ) mixes. For TRZ and BRZ mixes, there were significant differences in bulk specific gravity values for all three gyration levels. For the SMA mixes, there were significant differences at 15 and 50 gyrations, but the two methods provided similar results at 125 gyrations.

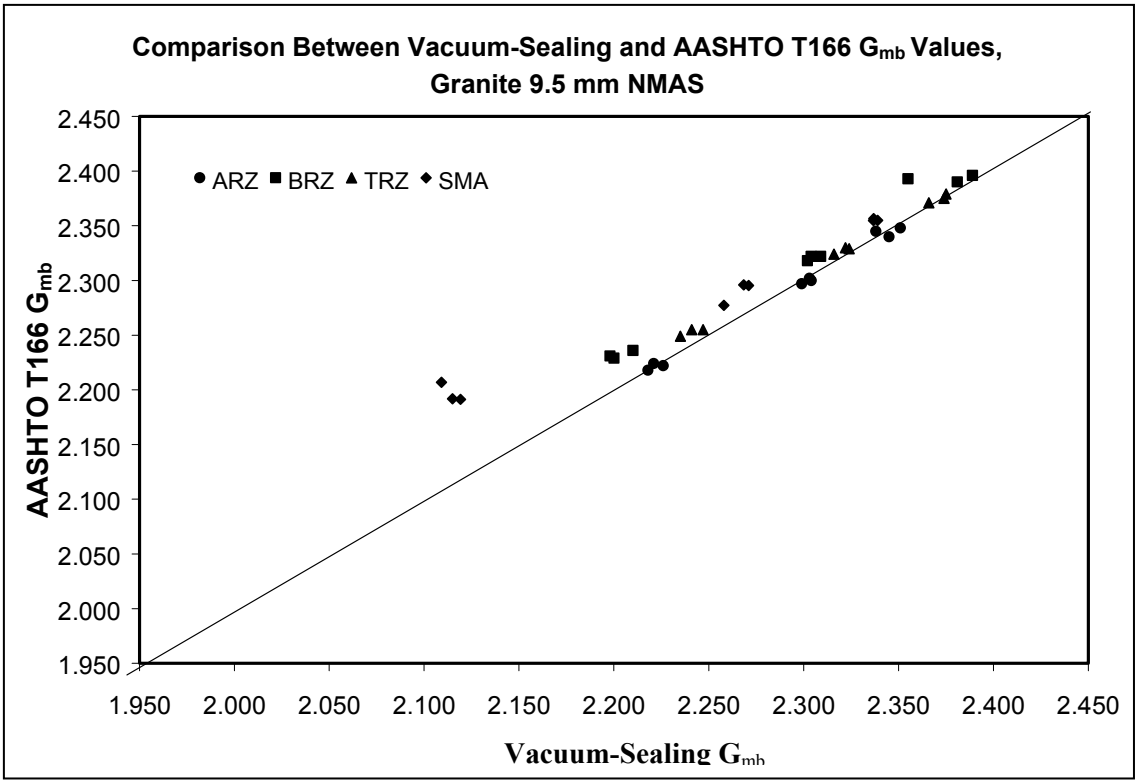

Figure 15: Comparison Between Vacuum-Sealing and AASHTO T166 Methods, 9.5 mm Granite

Figure 15 presents the comparisons between the two bulk specific gravity methods for the 9.5 mm NMAS granite mixes. Paired *t*-tests comparing bulk specific gravity results from the two methods were conducted. For the granite mixes, bulk specific gravity measurements on Superpave mix samples prepared at 125 gyrations were similar for both methods. For the BRZ and TRZ gradation shapes, the two methods

provided significantly different bulk specific gravity values at 15 and 50 gyrations. The two methods resulted in significantly different bulk specific gravity measurements at all three gyration levels for the SMA mixes.

Figures 16 and 17 illustrate comparisons between the two bulk specific gravity methods for the 12.5 mm SMA mixes. Paired *t*-tests were conducted to determine if the two methods provided significantly different results for the 12.5 mm NMAS SMA mixes. Figure 16 illustrates that for the limestone 12.5 mm NMAS SMA mixes, the two methods provide closer results at higher densities, but not similar. However, results of the paired *t*-tests showed that there were significant differences in bulk specific gravities at all three gyration levels. Figure 17 shows that the two methods also provided somewhat similar results at 50 and 125 gyrations for the granite mixes. Statistically, the results were similar; however, from a practical standpoint the two methods were different as the average difference in bulk specific gravities were 0.045 and 0.042 for the 50 and 125 gyration mixes, respectively. Both of these average differences in bulk specific gravity would have resulted in differences in air void contents of approximately 0.9 percent. Based upon the statistical and practical analysis of the 12.5 mm NMAS SMA mixes (both aggregate types), the two methods of measuring bulk specific gravity provided different results.

Comparisons between the vacuum-sealing and AASHTO T166 bulk specific gravity methods for the 19.0 mm NMAS mixes utilizing the limestone and granite aggregates are illustrated in Figures 18 and 19, respectively.

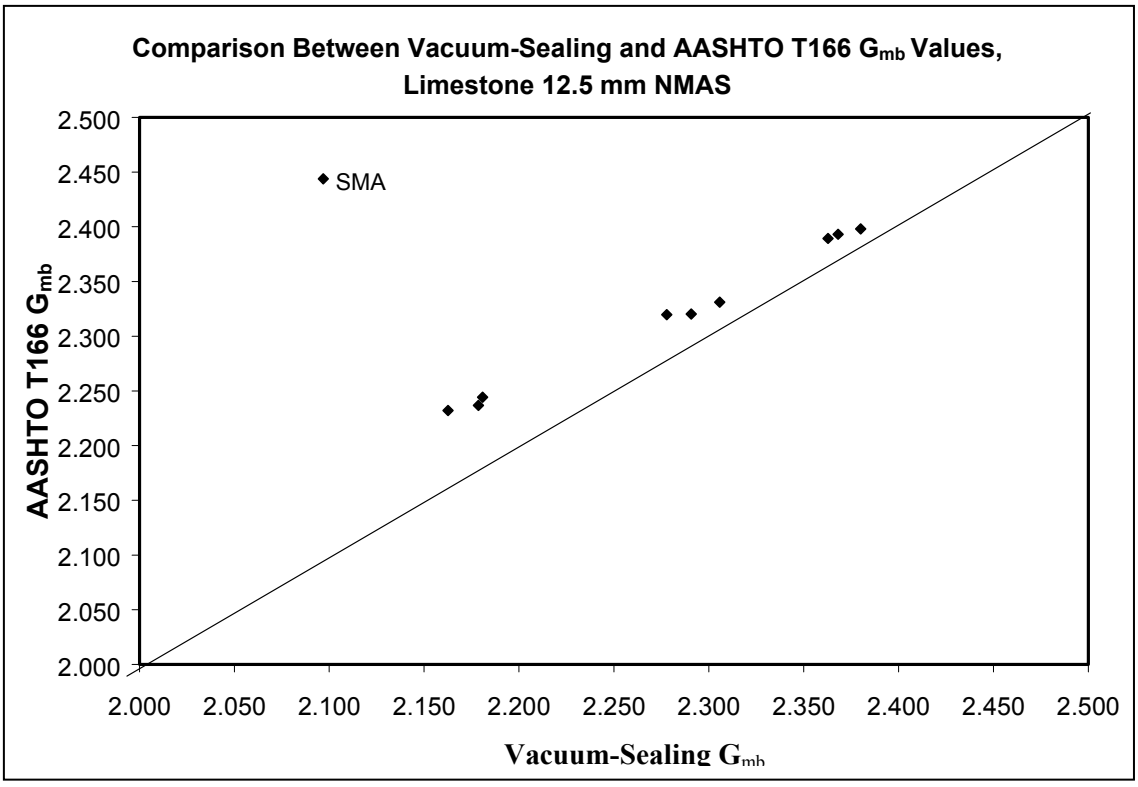

Figure 16: Comparison Between Vacuum-Sealing and AASHTO T166 Methods, Limestone 12.5 mm NMAS

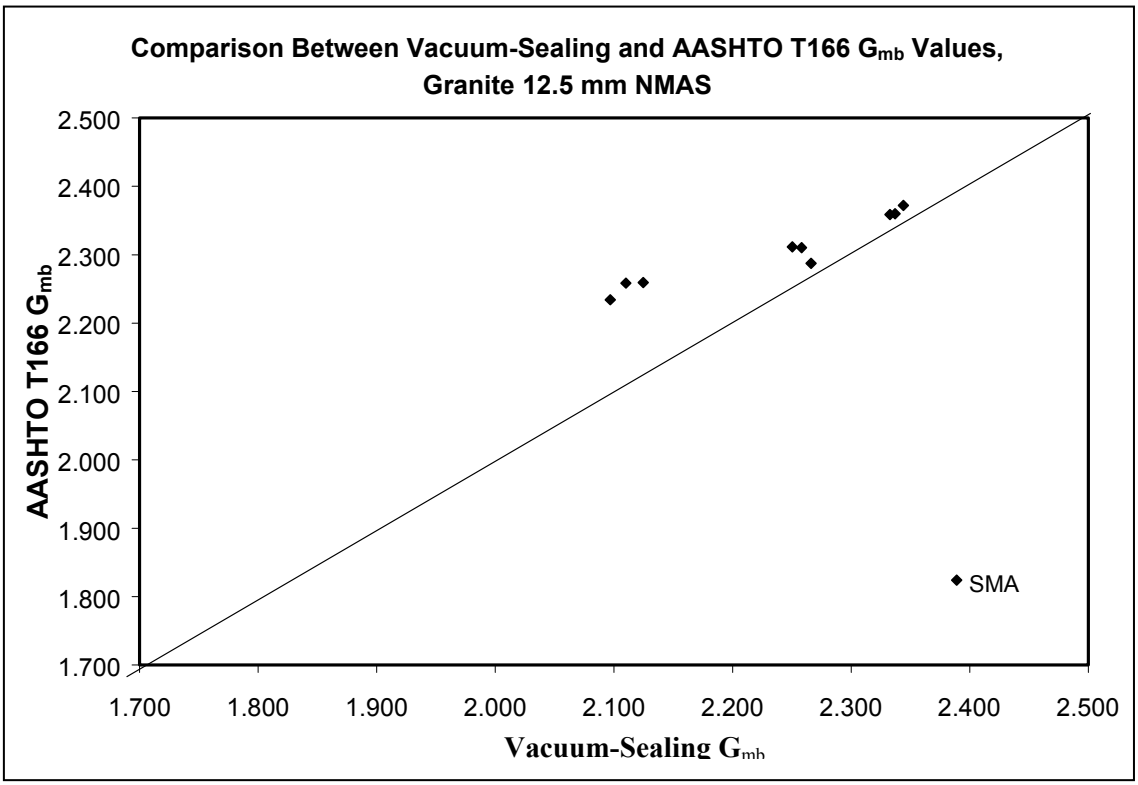

Figure 17: Comparison Between Vacuum-Sealing and AASHTO T166, Granite 12.5 mm NMAS

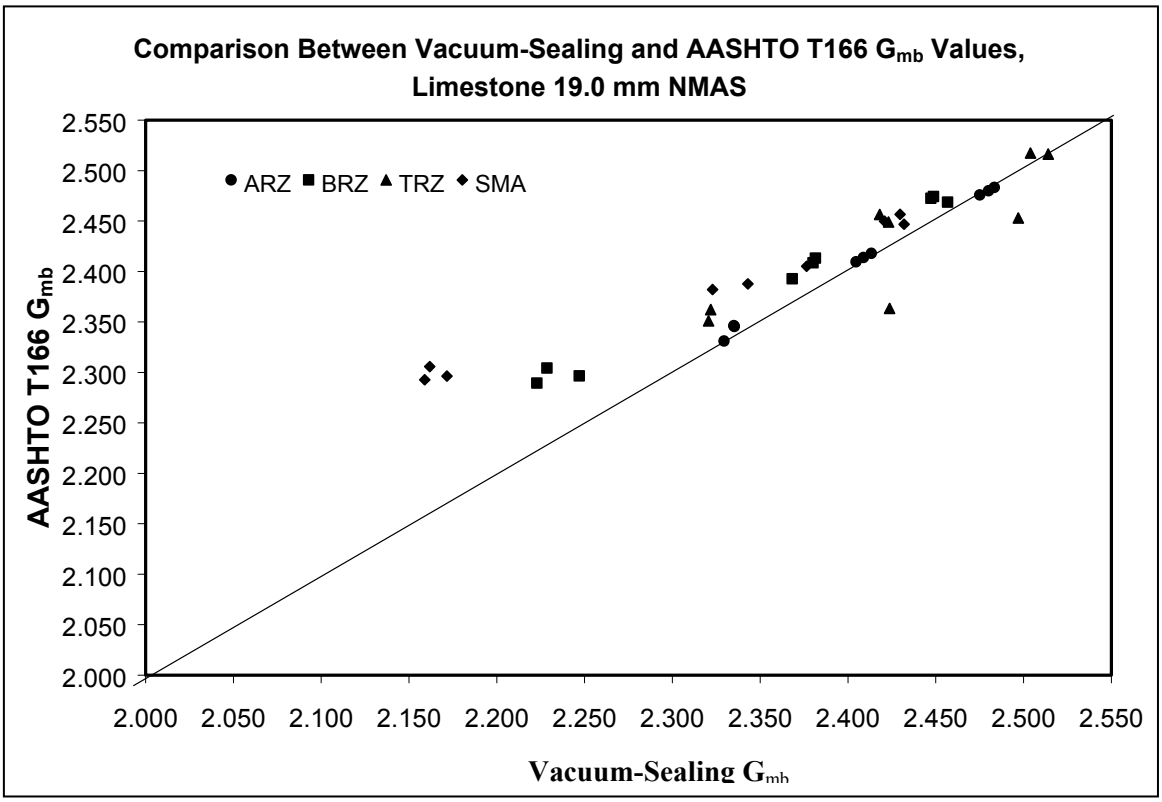

Figure 18: Comparison Between Vacuum-Sealing and AASHTO T166, Limestone 19.0 mm NMAS

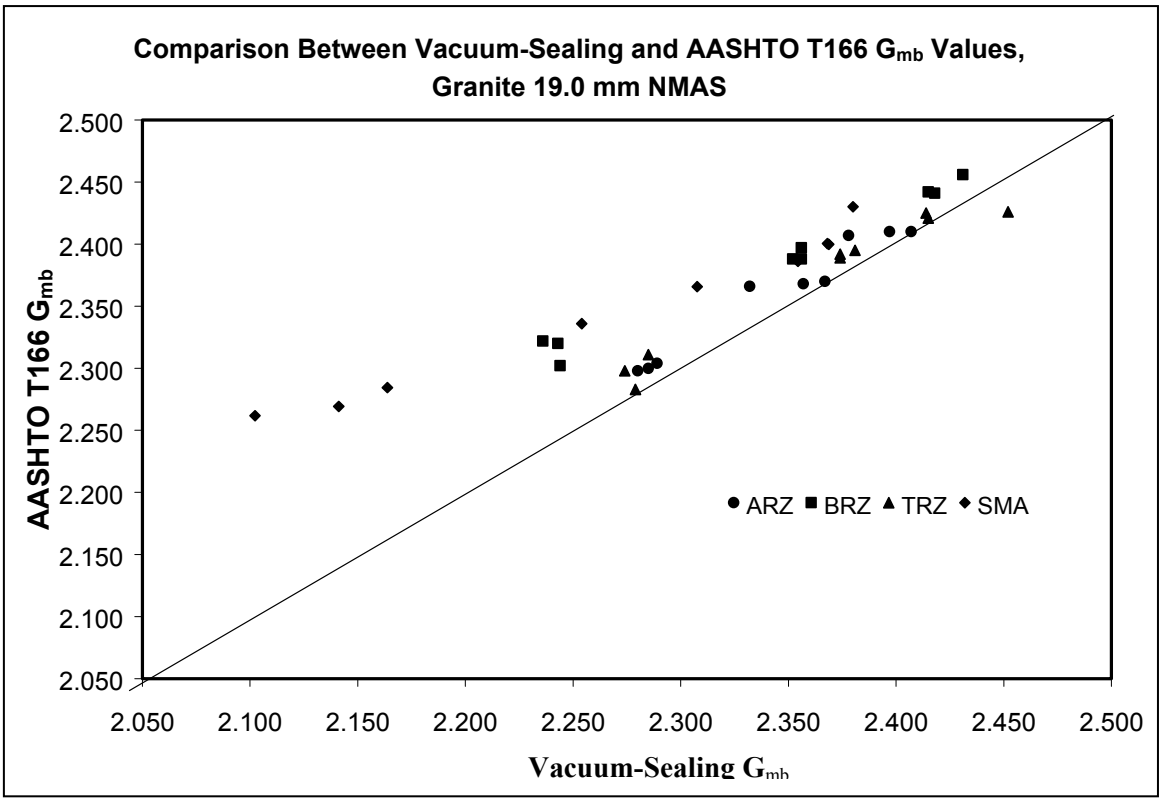

Figure 19: Comparison of Vacuum-Seal and AASHTO T166, Granite 19mm NMAS

Figure 18 illustrates that limestone mixes having ARZ and TRZ gradations compacted to 125 gyrations provided similar bulk specific gravity values when the two methods were compared. The two methods yielded similar bulk specific gravity values at all three gyration levels for the ARZ gradation mixes. For the BRZ and SMA mixes, the two methods provided significantly different bulk specific gravity values at all three gyration levels.

Figure 19 illustrates the comparisons between the vacuum-sealing and AASHTO T166 methods for the 19.0 mm NMAS granite mixes. Data are presented for the four gradation shapes evaluated for the 19.0 mm NMAS mixes: ARZ, BRZ, TRZ, and SMA. Figure 19 shows that for the two methods the ARZ mixes compacted to 50 and 125 gyrations provided similar results. Two other mixes, TRZ-15 gyrations and TRZ-125 gyrations also had strong comparisons between the two methods.

Figures 20 and 21 illustrate the comparisons between the vacuum-sealing and AASHTO T166 methods for the mixes containing the limestone and granite aggregates, respectively, having gradations with 37.5 mm NMAS. Results in Figures 20 and 21 show that the two bulk specific gravity methods did not compare well for the 37.5 mm NMAS mixes. In all cases, the AASHTO T166 method provided higher bulk specific gravity values.

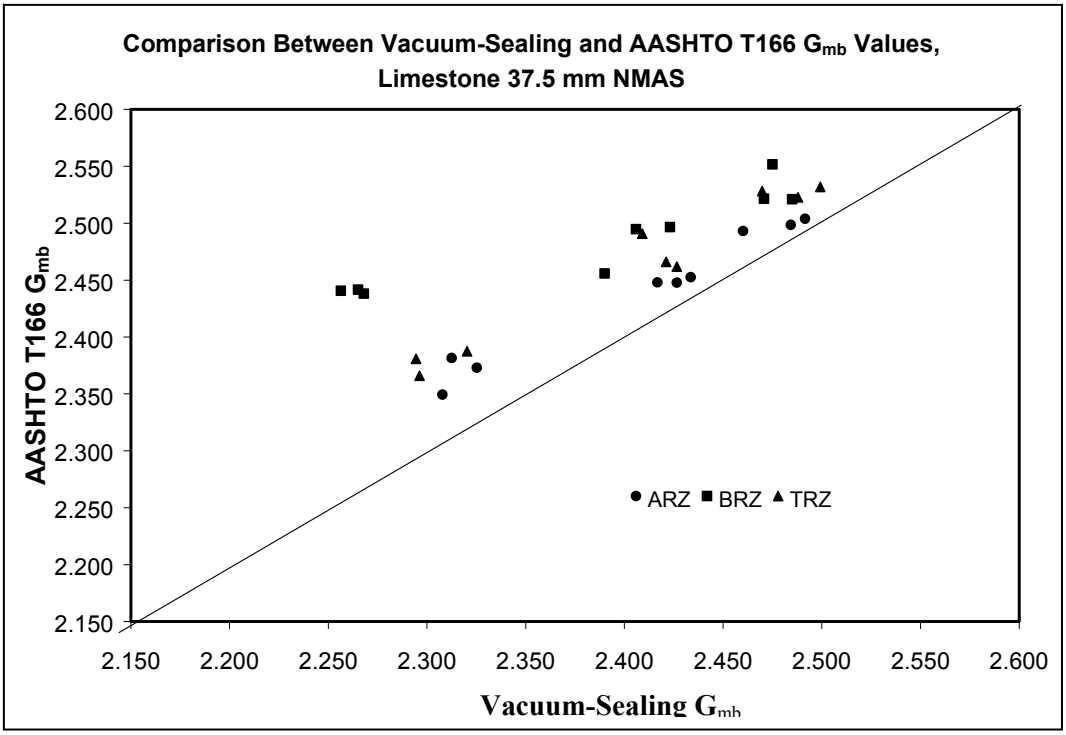

Figure 20: Comparison Between Vacuum-Sealing and AASHTO T166, Limestone 37.5 mm NMAS

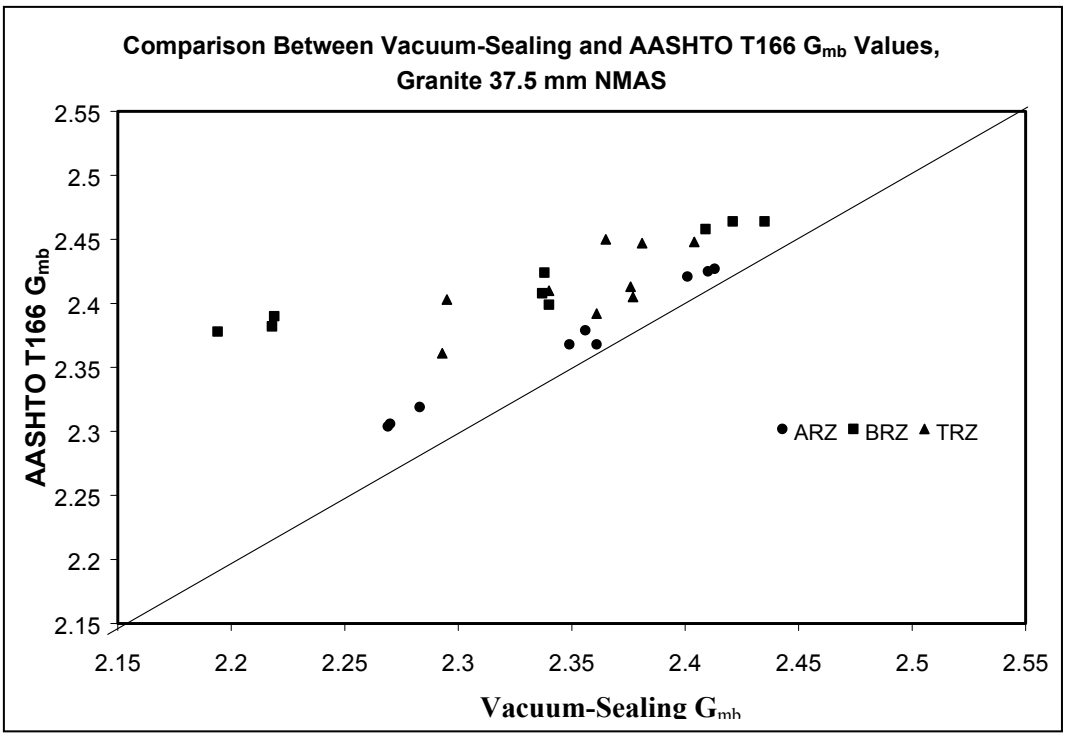

Figure 21: Comparison Between Vacuum-Sealing and AASHTO T166, Granite 37.5 mm NMAS

The preceding comparisons between the vacuum-sealing and AASHTO T166 bulk specific gravity methods showed that the two methods provided similar results (from a statistical and practical standpoint) only about 24 percent of the time. The NMAS which provided similar results the most often was 9.5 mm, while the gradation shape that provided similar results the most was the ARZ gradation. The gyration level which provided similar results the most often was 125. As noted previously, these mixes (9.5 mm, ARZ and 125 gyrations), are the mixes with the lowest water absorption levels (Figure 12) which is the condition for which the AASHTO T166 method is most accurate.

There are two possible reasons for the two methods providing significantly different results for larger NMAS mixes, coarser gradations, and lower gyration levels. The first possibility causing differences between the vacuum-sealing and AASHTO T166 methods would be that of surface texture on the sample. The vacuum-sealing method uses a vacuum to conform a plastic bag around the sample. If the bag does not tightly conform within the texture of the sample, then a portion of the sample's texture can be counted as part of the sample's volume. If this occurs, the sample's bulk specific gravity would be lower resulting in higher air voids. Figures 14 to 21 showed that for every instance where the two methods provided significantly different results, the vacuum-sealing method provided higher air voids.

Secondly, the combinations of larger NMAS, coarse gradations, and lower gyration levels provide for large voids within samples (though the overall volume would be typical). These large voids can be interconnected within the sample and therefore increase the potential for air voids that are interconnected to the sample's surface. As

stated previously, these large interconnected voids could provide avenues for water to quickly infiltrate the sample while submerged during AASHTO T166 testing. If the water can quickly infiltrate then it can also quickly exit the sample after it is taken out of the water. This would lead to errors in the AASHTO T166 method. The errors would lead to higher measured densities for samples (lower air voids).

A method for comparing the amount of surface texture accounted for with the vacuum-sealing method would be to compare the results from the vacuum-sealing and AASHTO T166 to the dimensional method on mixes with low water absorption. The difference between the dimensional and the other two bulk specific gravity methods should be the surface texture of the sample. Figure 22 illustrates the results of bulk specific gravity tests using the vacuum-sealing and AASHTO T166 methods versus results based upon the dimensional method for the 9.5 mm NMAS-ARZ-granite mixes. The amount of measured surface texture would be the difference between the line of equality and the results from the two methods. This figure shows that both the vacuum-sealing and AASHTO T166 methods provided a consistent measure of surface texture for these small NMAS fine-graded mixes. Both regression lines had slopes near 1.0 which would indicate little change in surface texture between the 15 and 125 gyration mixes.

This lack of change in surface texture was confirmed using a modified sand patch test to measure the macrotexture of samples. The test was similar to ASTM E965, "Measuring the Surface Macrotexture Depth Using a Volumetric Technique," except that the laboratory compacted samples were utilized. For this test, Ottawa sand was spread evenly over the face of a laboratory prepared sample. Knowing the mass of the sample before the sand was added and the mass of the sample with the evenly spread sand

allowed the amount of sand remaining within the surface texture (or macrotexture) of the sample to be determined. The amount of sand within the surface texture could then be converted to a volume using the bulk specific gravity of the Ottawa sand to represent the amount of macrotexture on the sample's surface.

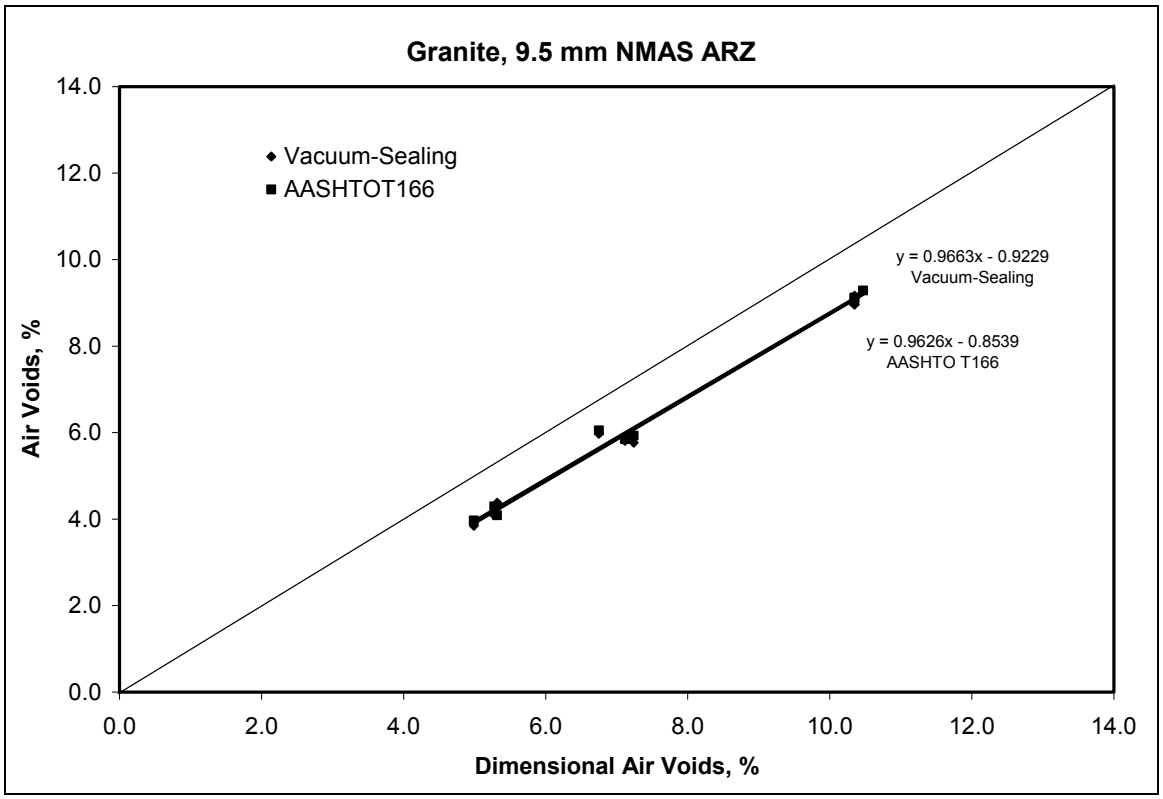

Figure 22: Evaluation of Surface Texture (Granite, 9.5 mm NMAS, ARZ)

The modified sand patch test was conducted three times on each of the 9 samples (three replicate samples at three gyration levels) meeting the 9.5 mm NMAS-ARZ-granite combination. Based upon the results, the surface texture measurements at 15, 50, and 125 gyrations were 26, 29, and 27 cm^3, respectively, which would indicate minimal differences in the amount of macrotexture at the three gyration levels.

At the other extreme, with respect to surface texture, would be a larger NMAS SMA mixture. Figure 23 shows a comparison between the dimensional results and results from the vacuum-sealing and AASHTO T166 methods for the 19.0 mm NMAS-SMA-granite combination. Samples of this combination compacted to 15 gyrations would also represent a worst case for the AASHTO T166 method because they should have large interconnected voids. Figure 23 shows a much larger difference between the dimensional results and the other two test methods than was observed for the finer 9.5 mm NMAS mixes. Neither of the regression lines have a slope near 1.0. Again, the difference between the two regression lines and the line of equality would be the amount

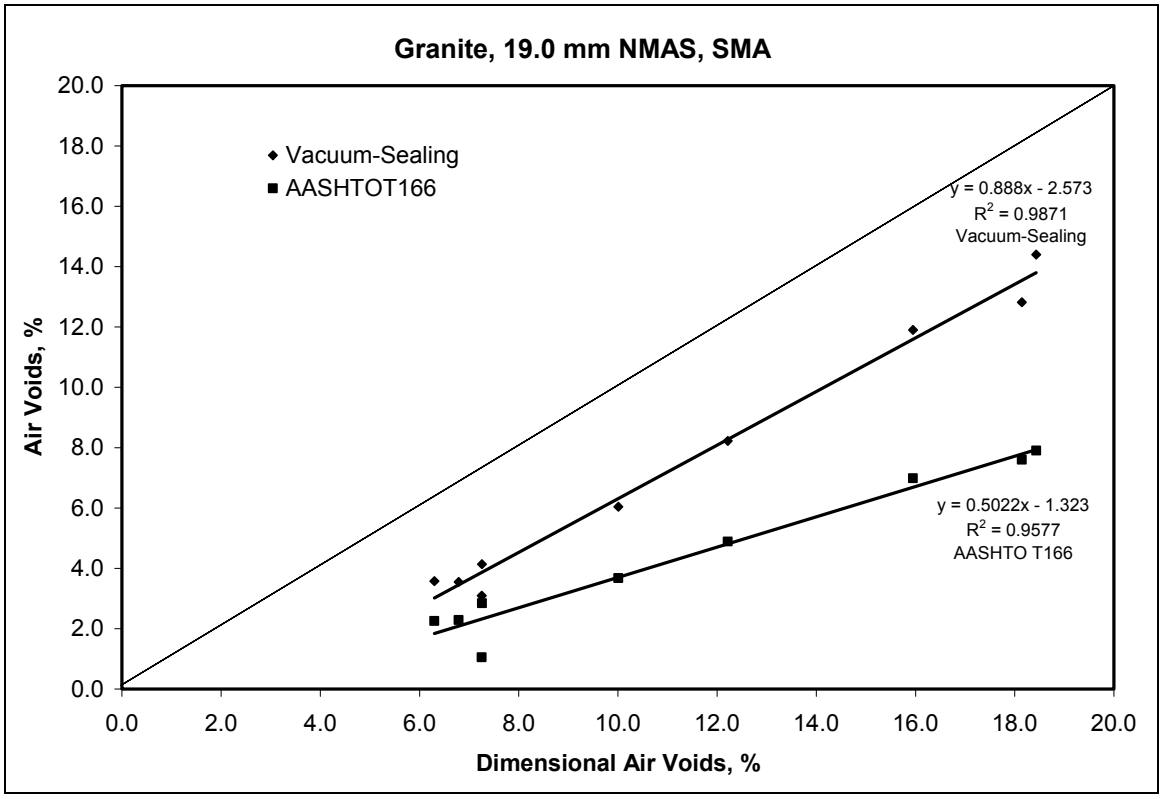

Figure 23: Evaluation of Surface Texture (Granite, 19.0 mm NMAS, SMA)

of surface texture. Based upon the regression lines, the AASHTO T166 method indicates more overall surface texture and a larger difference in surface texture between the 15 and 125 gyration samples (smaller slope than vacuum-sealing method).

The modified sand patch test was again conducted on the nine 19.0 mm NMAS-SMA-granite samples. Results of this testing for the 15, 50, and 125 gyration samples were 129, 100, and 83 cm^3, respectively. These results show that the macrotexture was affected by the amount of compactive effort used to compact the samples (or air voids). However, the question still remains, which of the two methods (vacuum-sealing or AASHTO T166) better predicted the amount of surface texture and, hence, bulk specific gravity?

The modified sand patch results were used to estimate the total amount of macrotexture for each of the nine 19.0 mm NMAS-SMA-granite samples. This was accomplished by determining the amount of macrotexture per unit area based upon the sand patch test on a single face of a sample. Next, the total surface area of the sample was estimated by adding the area of the two sample faces and the total perimeter of the sample. The macrotexture per unit area was then applied to the total surface area of the sample to estimate the total amount of macrotexture on the sample. Results of these calculations are presented in Table 16. Also included within this table are the volumes calculated from the bulk specific gravity results (all three methods) and differences in volumes between the dimensional method and the other two methods. Again, these differences should be estimates of surface texture on a sample. The method for which the estimated surface texture better approximates the measured surface texture (depending upon the method) would be a better predictor of bulk specific gravity.

Table 16: Evaluation of Surface Texture for 19.0 mm NMAS-SMA-Granite Samples

Gyration	Rep.	Dim. Volume, cc (Dvol)	Vacuum-Sealing Volume, cc (VSvol)	T166 Volume, cc (Tvol)	Macrotexture on Single Face, cc	Dvol-VSVol	Dvol-Tvol	Est. Total Surface Texture, cc
15	1	2196.6	2062.3	1945.9	27.1	134.2	250.6	144.2
15	2	2142.6	2044.2	1936.1	22.6	98.5	206.5	118.2
15	3	2195.6	2092.2	1944.6	23.6	103.4	251.0	125.4
50	1	2026.8	1939.7	1899.7	19.2	87.1	127.0	96.9
50	2	2087.3	1999.1	1950.1	21.7	88.1	137.2	111.8
50	3	2115.0	2022.9	1952.0	17.9	92.0	163.0	93.1
125	1	2079.3	2009.5	1983.6	16.2	69.8	95.8	83.4
125	2	2066.4	2008.1	1981.0	16.5	58.4	85.4	84.7
125	3	2088.9	2020.8	1994.0	15.7	68.0	94.9	81.1

Figure 24 illustrates the relationships between the measured surface texture (differences in volumes) and the estimated total surface texture from the modified sand patch test for the nine samples of the 19.0 mm NMAS-SMA-granite combination. This figure shows that the results of the vacuum-sealing method closely tracked the estimated amount of surface texture from the modified sand patch test. Results from the vacuum-sealing test method (difference in sample volume between dimensional and vacuum-sealing) fell almost on the line of equality and had a slope of approximately 1.0. Results from the AASHTO T166 method were near the line of equality at the lower values of surface texture (125 gyration samples) but deviated from the line of equality at higher levels of surface texture (15 gyration samples). This would indicate that the vacuum-sealing method does an adequate job of taking into account the surface texture of a sample when air voids are low. Also, results from AASHTO T166 greatly overestimated the amount of surface texture at higher overall air void contents (15 gyration samples). Consequently, if AASHTO T166 is overestimating the amount of surface texture, then it must also be underestimating the amount of internal air voids. Therefore, based upon this

analysis of the surface texture data, the vacuum-sealing method does a better job of estimating the amount of surface texture on a sample and, hence, does a better job of estimating the internal air voids for samples at low densities.

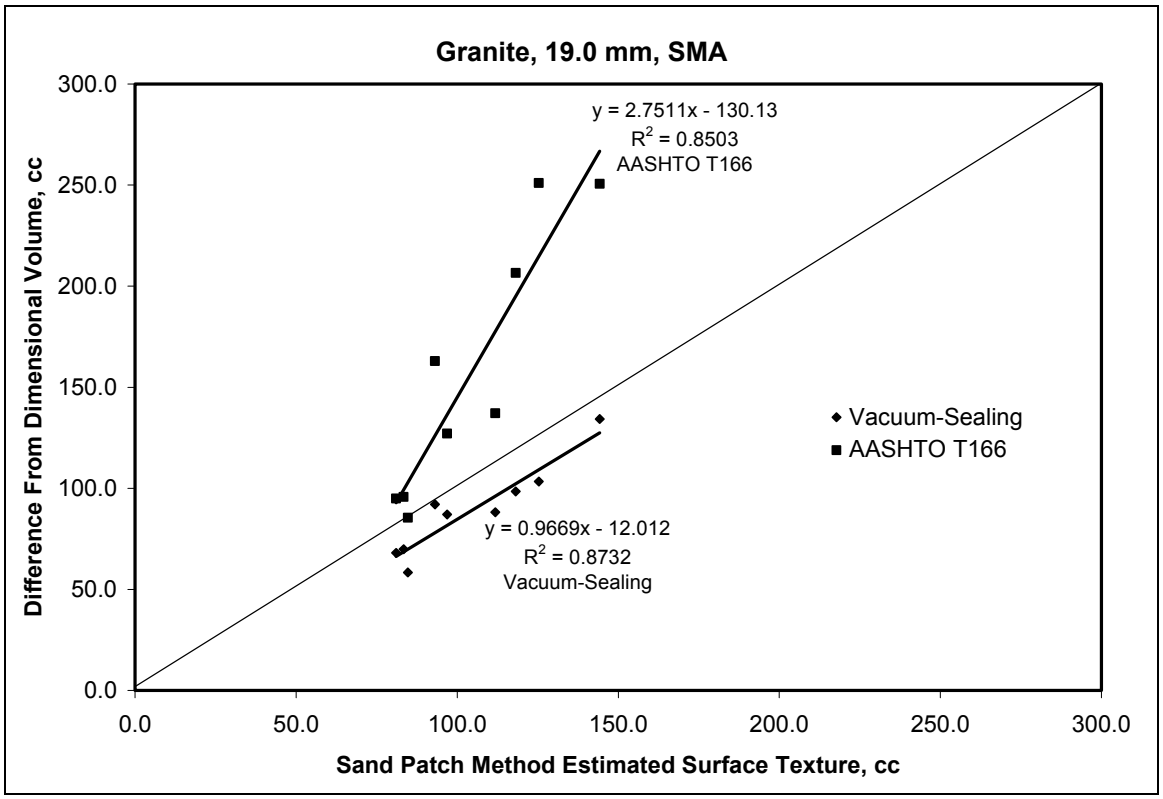

Figure 24: Comparisons of Measured and Estimated Surface Textures

The second possibility discussed for the difference between the vacuum-sealing and AASHTO T166 methods was that of excessive amounts of water entering and exiting a sample. A method of determining whether an excessive amount of water enters a sample and leads to errors in AASHTO T166 testing would be to evaluate the amount of water absorption. This analysis would not provide an exact measure of the volume of water that enters and exits a sample during AASHTO T166, but rather provides a measure of the potential. As water absorption increases, the number and size of air voids

interconnected to the surface would also increase. For this analysis, air void contents were utilized instead of bulk specific gravities because of the differences in aggregate specific gravities between the mixes. Also, mixtures were categorized by only gradation shape instead of NMAS, gradation shape, and aggregate type.

Figure 25 illustrates the relationship between air voids and water absorption for both bulk specific gravity methods for mixes having ARZ gradations. Data shown in this figure represent NMASs of 9.5, 19.0 and 37.5 mm. This figure shows that the two methods provided similar air void contents at low water absorptions (as was shown previously). However, at higher levels of water absorption the two methods begin to diverge. The standard method for AASHTO T166 indicates that the method is only applicable at water absorptions of 2.0 percent and below. Figure 25 shows that at 2.0 percent water absorption, the two methods resulted in a difference of 1.0 percent air voids (8.7 percent for the vacuum-sealing method and 7.7 percent for AASHTO T166). This difference is greater than would be desired.

Based upon the discussion of the problems with the AASHTO T166 method earlier within this report, Figure 25 is logical. At high densities (low air voids), there are very low water absorptions and the two methods provide similar results. However, at lower densities there are higher water absorption values and differences between the two methods. Because of the vacuum-sealing test method, conforming the plastic bag to the sample, it can be surmised that if the method works at high densities, it also works at lower densities.

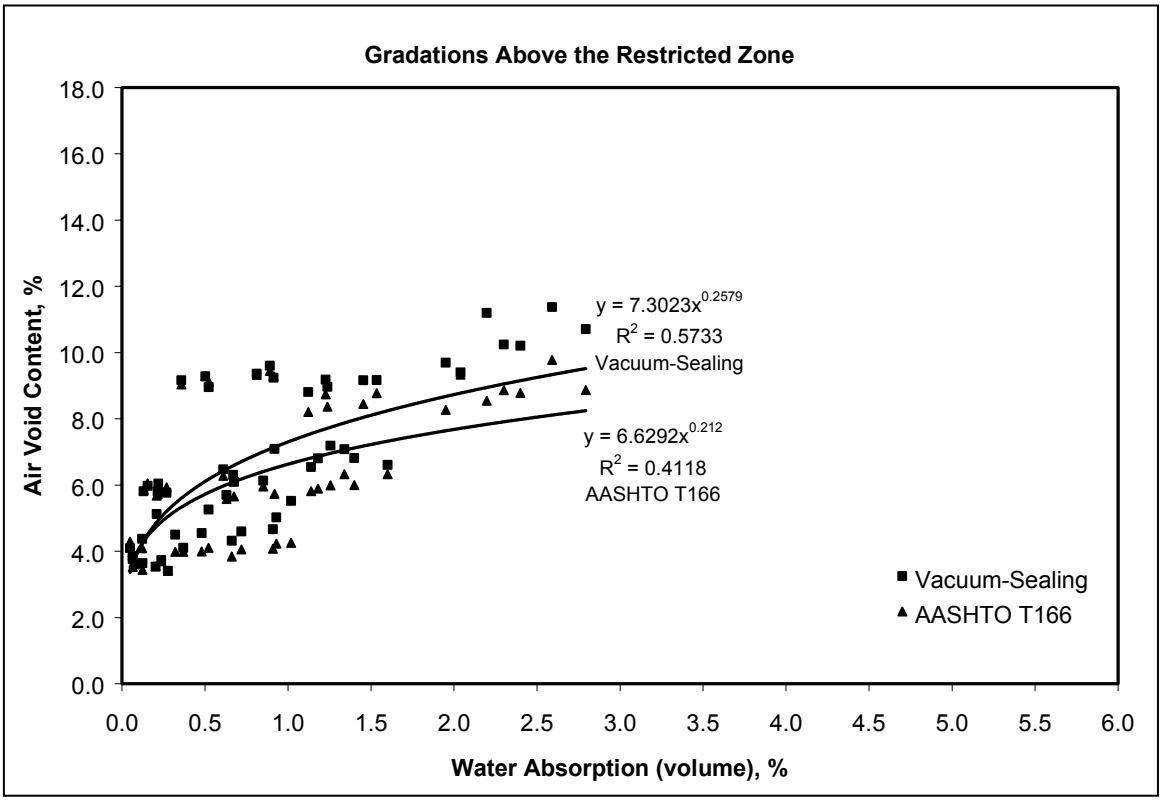

Figure 25: Relationship Between Water Absorption and Air Voids, ARZ mixes

Now the question that must be answered is whether the two methods provide similar results over the range of water absorption levels encountered. Figure 25 shows that the two methods provided similar results for mixes having ARZ gradations.

The relationship between air voids and water absorption for mixes having BRZ gradations is illustrated in Figure 26. Once again, this figure shows that at very low levels of water absorption, the two methods resulted in similar air void contents. However, as the level of water absorption increased the air void contents from the two methods diverged. This figure shows that the two methods diverged at approximately 0.4 percent water absorption, which indicates the two methods provided significantly

different results at water absorption values above 0.4 percent. This level of water absorption at which the two methods diverged was also found by Cooley *et al* (*4*) for coarse-graded mixes. For the BRZ mixes, the 0.4 percent water absorption level corresponded to approximately 3.5 percent air voids. This level of air voids is below the typically used design air void level of 4.0 percent. This would indicate that the use of the vacuum-sealing method during mix design would have resulted in a higher asphalt binder content. At 4 percent air voids determined by the vacuum-sealing method, the difference in air voids determined by the two methods was 0.7 percent. Based upon this difference in air voids, the use of the vacuum-sealing method would have resulted in approximately 0.3 percent more asphalt binder than when using AASHTO T166.

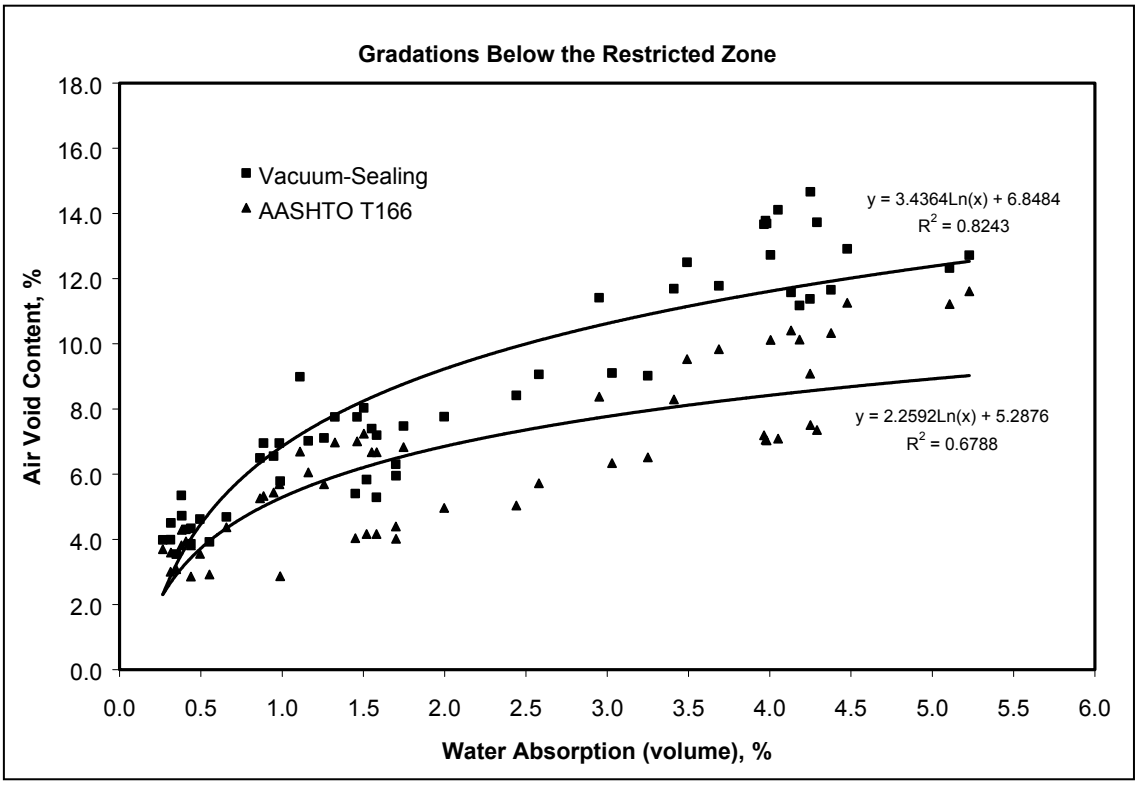

Figure 26: Relationship Between Water Absorption and Air Voids, BRZ mixes

Figure 27 illustrates the relationship between air voids and water absorption for the mixes having TRZ gradations. Similar to the ARZ and BRZ relationships, this figure shows that at low levels of water absorption (high densities) the vacuum-sealing and AASHTO T166 methods yielded similar results. However, at higher levels of water absorption the two methods diverge with the vacuum-sealing method providing a higher air void content. Figure 27 illustrates that the two methods yielded similar results up to about 0.4 percent water absorption. Above this level of water absorption, the vacuum-sealing method resulted in higher air void contents. 0.4 percent water absorption level corresponded to approximately 3.5 percent air voids for both methods. This level of air voids is below the typically used design air void level of 4.0 percent. This would indicate that the use of the vacuum-sealing method during mix design would have resulted in a higher asphalt binder content.

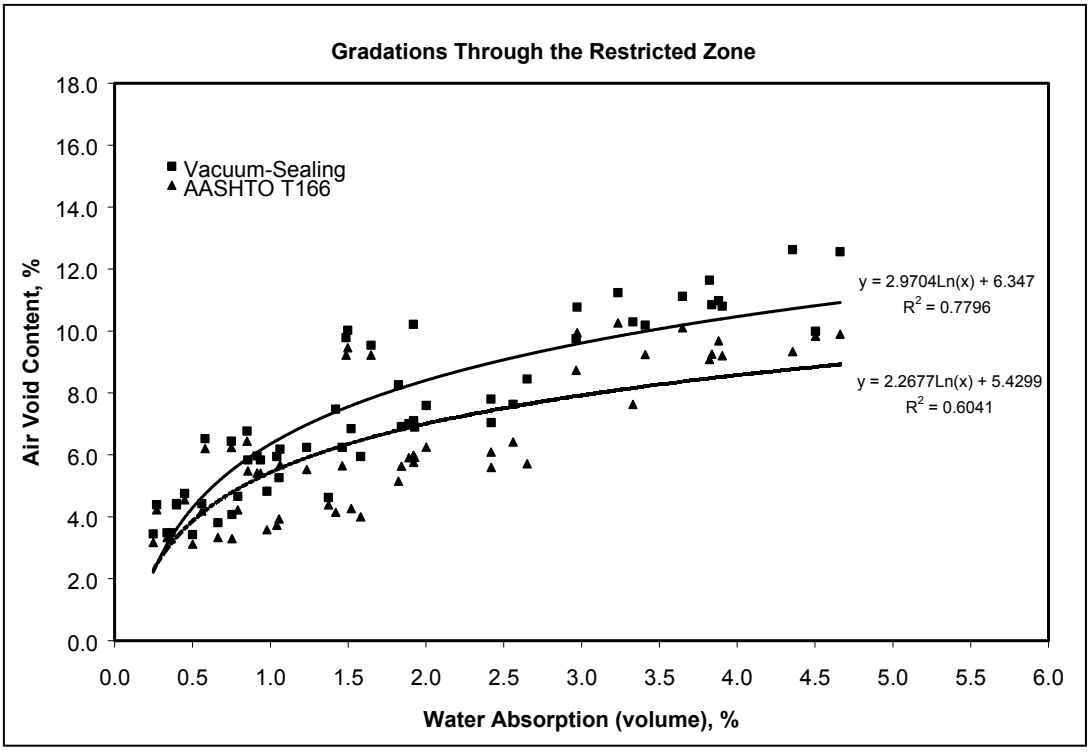

Figure 27: Relationship Between Water Absorption and Air Voids, TRZ mixes

Figure 28 illustrates the relationship between water absorption and air voids for mixes having a SMA gradation. Both relationships had strong R^2 values as both were above 0.80. This figure shows that the two bulk specific gravity methods yielded similar results at very low water absorption values. This figure shows that for the SMA mixes, the two methods diverged at approximately 0.2 percent water absorption. This level of water absorption corresponded to an air void content of approximately 2 percent which is less than typical design air voids. At 4 percent air voids for the vacuum-sealing method, the average difference in air voids between the two methods was 1.0 percent. This difference in air voids at the design level would have resulted in about 0.4 percent more asphalt binder if the vacuum-sealing method was used instead of AASHTO T166.

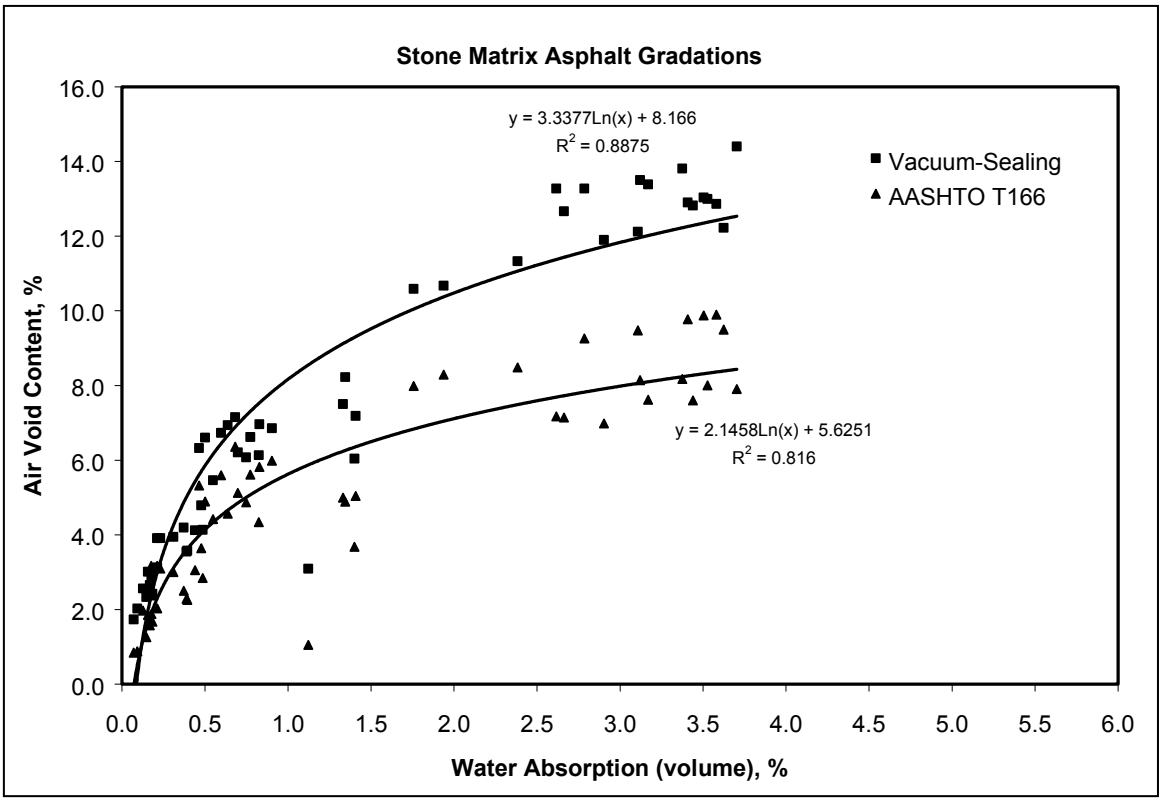

Figure 28: Relationship Between Water Absorption and Air Voids, SMA mixes

6.1.1 Summary of Comparisons Between Bulk Specific Gravity Methods for Laboratory Specimens

The analyses comparing the vacuum-sealing and AASHTO T166 methods suggest that the vacuum-sealing method is more accurate for low density samples. The relationships between water absorption and air void contents suggested that the AASHTO T166 method was accurate for all water absorption levels encountered for mixes that were fine-graded (ARZ). However, for mixes having gradations near the maximum density line (TRZ) or coarser (BRZ and SMA), the level of water absorption that AASHTO T166 no longer becomes accurate was between 0.2 and 0.4 depending upon the gradation. These values were much lower than anticipated; therefore, an additional study was conducted to further evaluate the water absorption level at which AASHTO T166 becomes inaccurate.

This experiment involved evaluating the effect of time to achieve the saturated surface dry (SSD) condition on water absorption. Times taken to achieve the SSD condition were 6 (as fast as could be achieved), 10, 15, 20, 30, and 60 seconds. The premise of the experiment was that samples having a large proportion of interconnected voids to the surface of a sample should show decreasing levels of water absorption as the time to achieve the SSD condition increases. Results of this side experiment should provide a level of water absorption that leads to increased potential for errors during AASHTO T166 testing. If a level of water absorption was identified at which the potential for errors during AASHTO T166 testing increased, the standard could be changed to indicate a new critical value of water absorption (instead of the current 2.0 percent).

A total of 40 samples were selected from the 216 used in the primary experiment. These samples included the all of the NMASs, gradation shapes, aggregate types, and gyration levels evaluated. Water absorption values ranged from 0.06 percent to 5.23 percent. Information on the 40 selected mixes is provided in Appendix A. For analysis, the different mixtures were grouped by gradation shape (ARZ, BRZ, TRZ, and SMA) and level of water absorption. Categories for water absorption were less than 0.5 percent, 0.5 percent to 1.0 percent, 1.0 percent to 1.5 percent, 1.5 percent to 2.0 percent, 2.0 percent to 2.5 percent, and above 3.0 percent.

Results of this side experiment for mixes having an ARZ gradation are illustrated in Figure 29. The y-axis for this figure is the difference in air voids from the initial (6 seconds) determination of SSD. The x-axis represents the time taken to achieve the SSD condition. Also shown on the figure is a horizontal line at 0.25 percent air voids. This air void content was deemed a critical air void content by Al-Khaateeb *et al* (*11*) because it resulted in an increase of 0.1 percent asphalt binder content during design.

Figure 29 illustrates that at water absorption levels less than 1.5 percent, the air void content level remained basically unchanged. Only the absorption category of 1.5 to 2.0 percent was above the critical change in air voids of 0.25 percent. However, this category did not reach the critical level until a time of 30 seconds to achieve the SSD condition. Results illustrated in Figure 29 suggest that at water absorption levels less than 2.0 percent the AASHTO T166 method is accurate for fine-graded mixes. This is similar to the results shown in Figure 25.

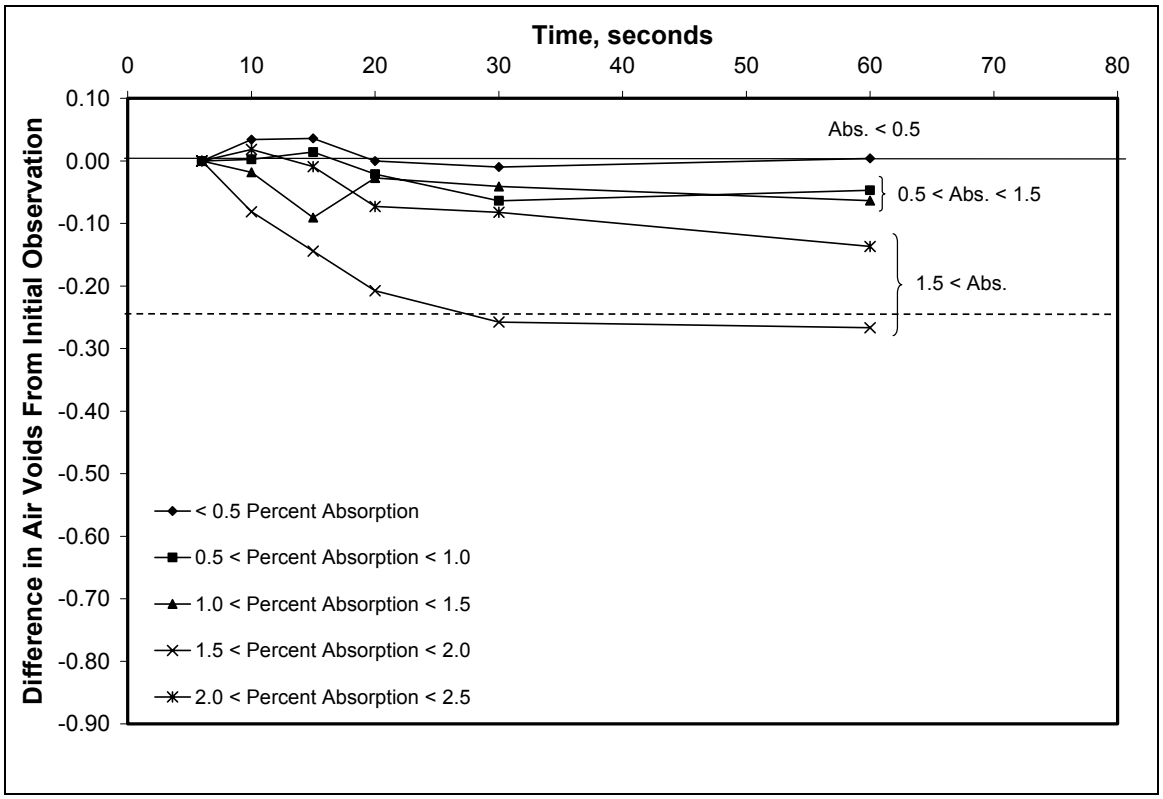

Figure 29: Results of Time To Reach SSD Condition, ARZ Mixes

Figure 30 illustrates the relationship between the change in air voids and time to achieve SSD for mixes having coarse gradations (BRZ). Based upon these results, mixes having water absorption levels greater than 1.0 percent exceeded the critical change in air voids while mixes having water absorptions less than 1.0 percent did not. Most of the mixes having water absorption levels above 1.0 percent resulted in changes in air voids greater than the 0.25 percent at times less than 15 seconds.

The effect of time to achieve the SSD condition on the change in air voids for mixes having gradations passing near the maximum density line (TRZ) is illustrated in Figure 31. Similar to the BRZ gradation mixes, this figure shows that once the level of water absorption increased above 1.5 percent the critical air void level was exceeded.

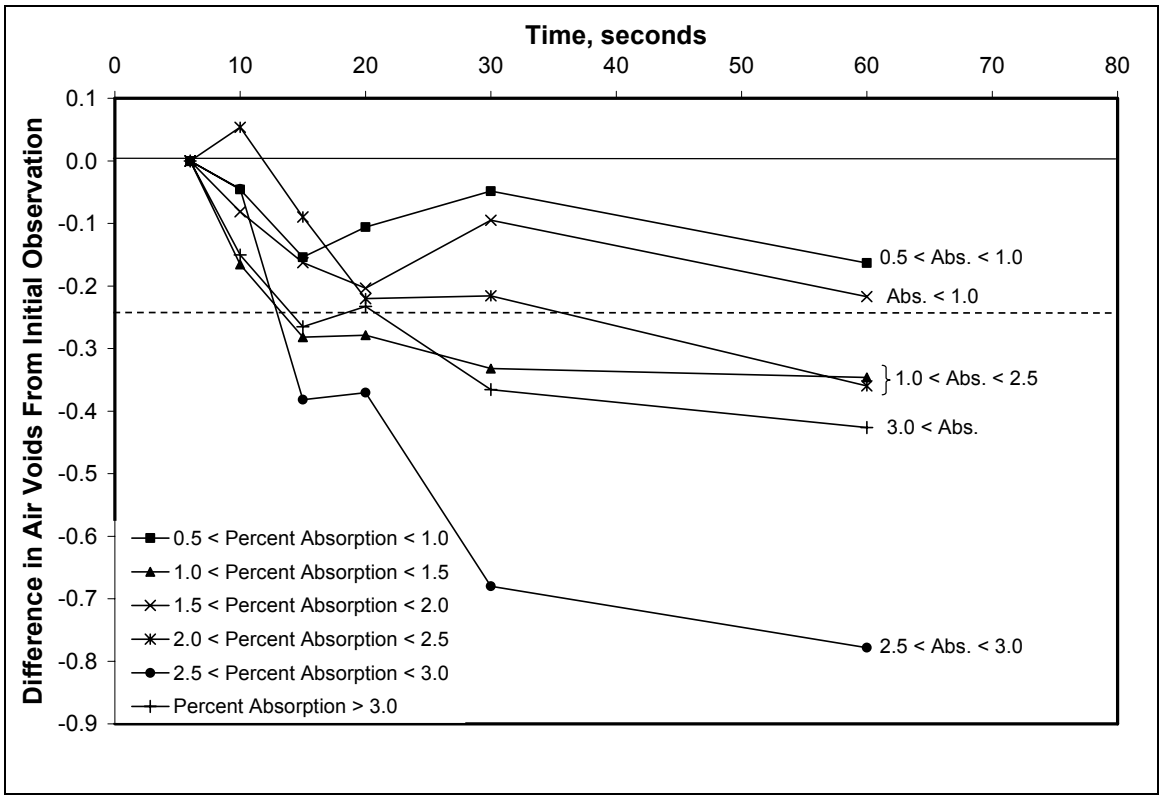

Figure 30: Results of Time To Reach SSD Condition, BRZ Mixes

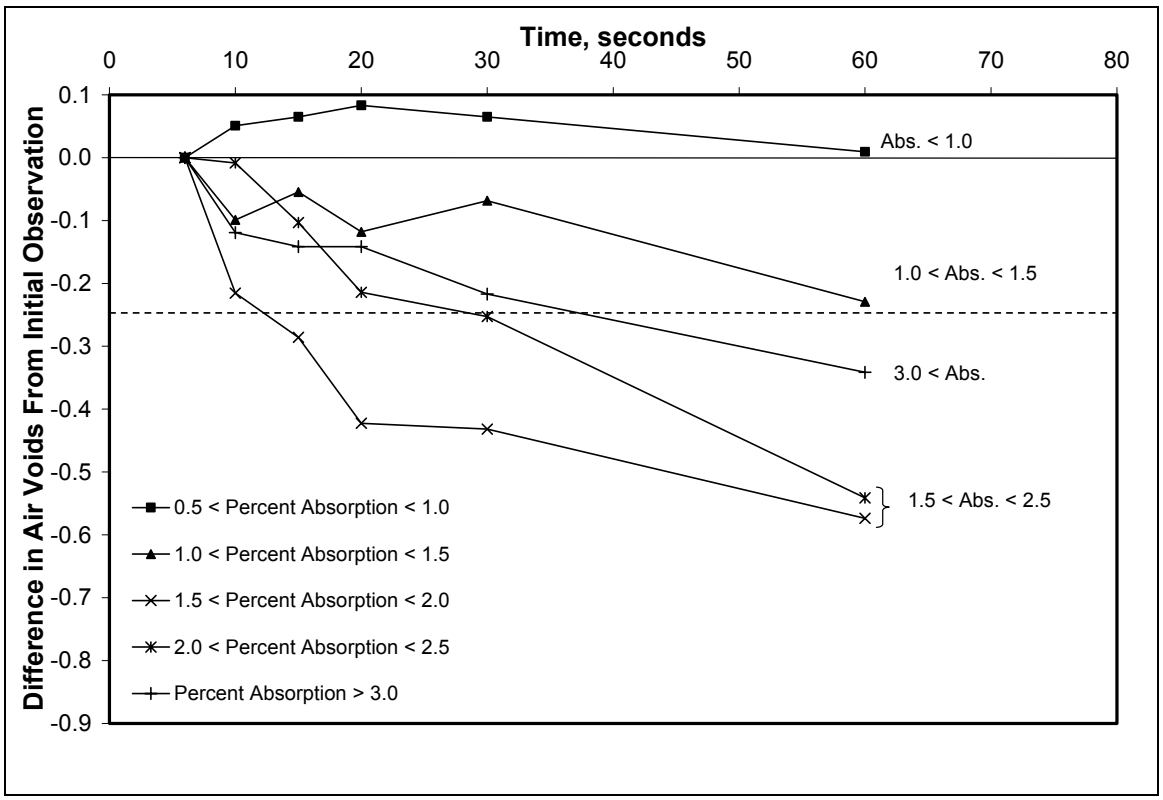

Figure 31: Results of Time To Reach SSD Condition, TRZ Mixes

These results would suggest that a critical level of water absorption for mixes having gradations passing near the maximum density line (TRZ) would be 1.5 percent.

Figure 32 illustrates the results of the time to achieve the SSD condition for the SMA mixes. This figure shows that there were large differences in air voids at water absorption levels above 1.0 percent. However, at water absorption levels below 1.0 percent, the data did not pass the critical air void content of 0.25 percent.

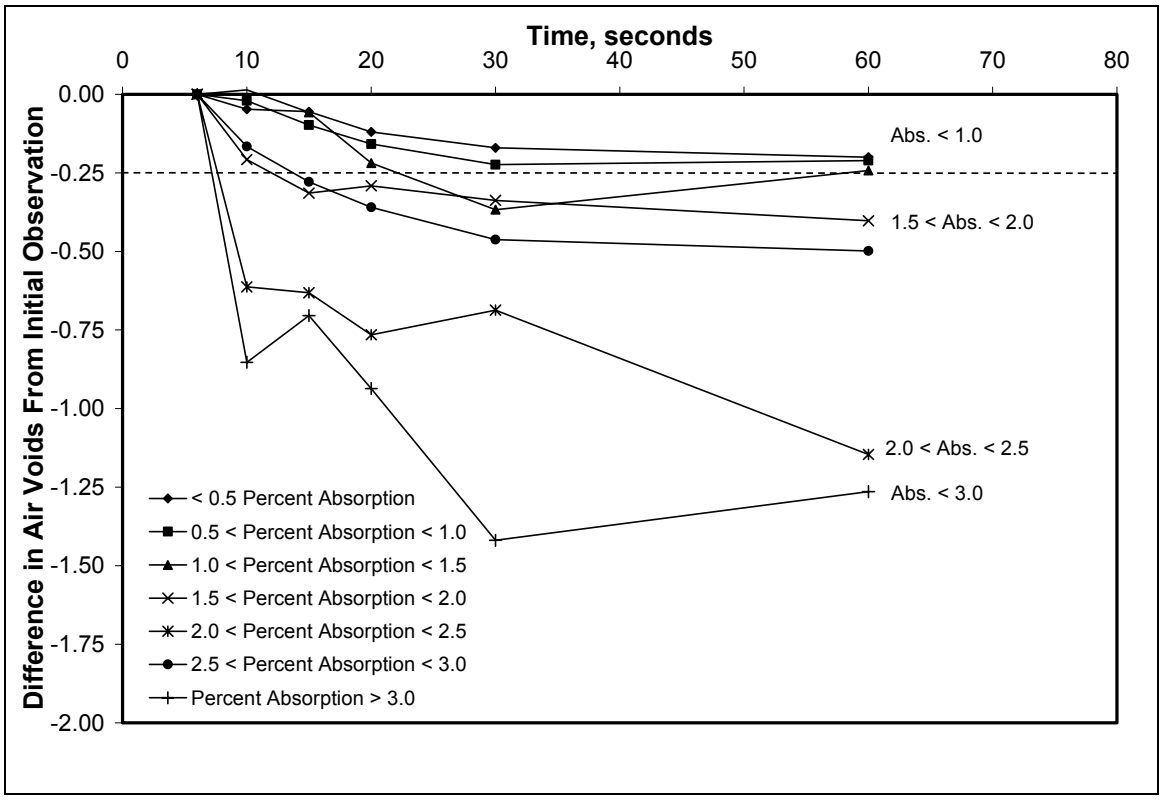

Figure 32: Results of Time To Reach SSD Condition, SMA Mixes

Results of the primary experiment and the side experiment suggest that the AASHTO T166 method is not accurate for mixes having gradations near the maximum density line and coarser when water absorption levels are at 2.0 percent. From the main experiment, the results suggested that the critical level of water absorption was 0.4 percent for mixes having BRZ and TRZ gradations, and 0.2 percent for SMA mixes.

These are all relatively small amounts of water absorption. From the side experiment, the critical levels of water absorption were 1.5, 1.0, and 1.0 percent for the TRZ, BRZ, and SMA gradation mixes. These values seem more reasonable; however, the problem still remains that the critical levels are different for each of the gradation shapes.

6.2 Analysis of Field Compacted Samples

Included within this portion of the study were the cores obtained during the Task 5 field validation experiment. Only the vacuum-sealing and AASHTO T166 test methods were analyzed, as they were shown most accurate during the laboratory phase of this experiment. Figure 33 illustrates the relationship between air voids determined from the two methods for all cores obtained during Task 5. This figure illustrates that at air void contents less than about 5 percent, the two methods provided approximately similar results. Above 5 percent air voids, the vacuum-sealing method resulted in higher air void contents. As air voids increased, the two methods diverged.

Initial analysis of the data compared the vacuum-sealing device versus that of the AASHTO T166 for these field compacted samples. Similar to the analysis conducted for the laboratory prepared samples, mixes having low water absorption levels and small NMAS were utilized in this analysis. These mixes were selected because the AASHTO T166 method is believed to be accurate at low water absorption levels.

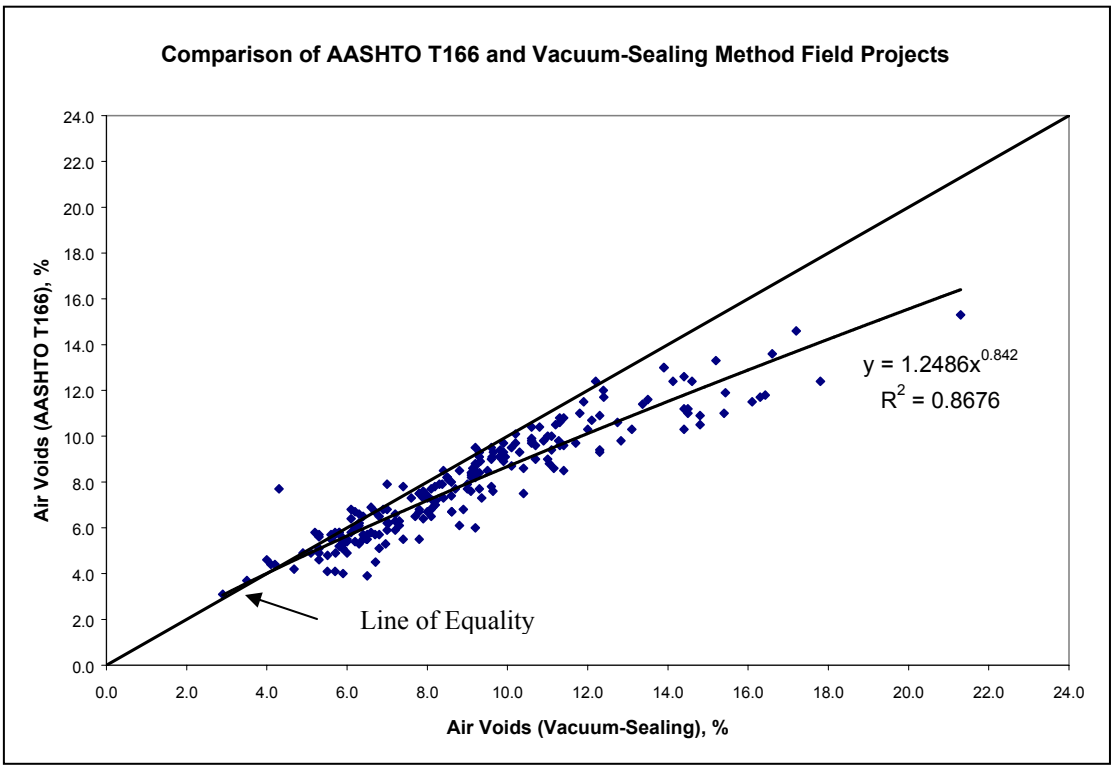

Figure 33: Comparison Between AASHTO T166 and Vacuum-Sealing Methods, Field Projects

A paired t-test was conducted on data from mixes having a 9.5 or 12.5 mm NMAS and water absorption levels less than 0.5 percent. A total of 44 cores were included in the data set. Results of this analysis indicated that the two methods provided similar results for these low absorption mixes (t-statistic=0.486, t-critical=2.017, and p-value=0.629).

Figure 34 illustrates the comparison between the two methods at water absorption levels below 0.5 percent. This figure confirms that the two methods resulted in similar air void contents. The average air void content using the AASHTO T166 method was 6.89 percent and the average air void content with the vacuum-sealing method was 6.82

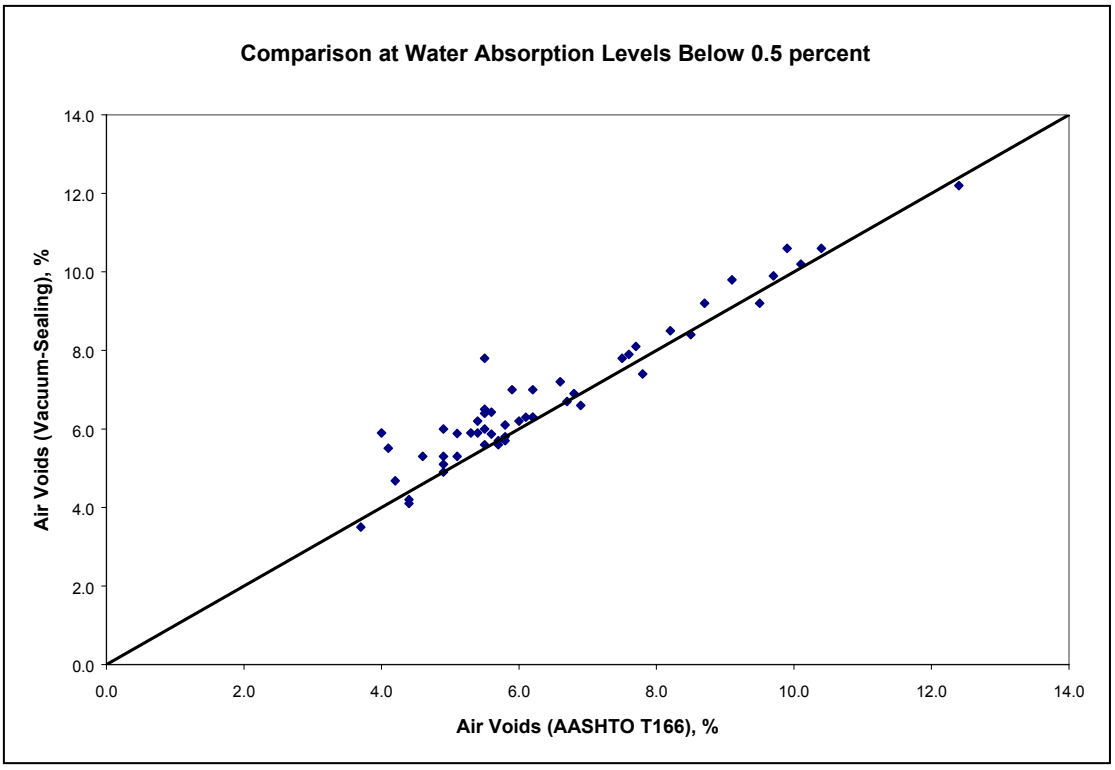

Figure 34: Comparison of Two Methods at Water Absorption Levels Less than 0.5 Percent

percent. Therefore, based upon this analysis the vacuum-sealing method does provide an accurate measure of bulk specific gravity.

The next analysis was to categorize all of the mixes according to their water absorption level and conduct paired *t*-tests to compare the vacuum-sealing and AASHTO T166 methods. The first category was all mixes having a water absorption level less than 0.5 percent. A total of 58 cores met this requirement. Results of the paired *t*-test for this category are presented in Table 17. The results show that the two bulk specific gravity methods resulted in similar air void contents when water absorption levels were less than 0.5 percent. Average air voids resulting from the AASHTO T166 method were 6.43 percent, while the average air voids resulting from the vacuum-sealing method were 6.66

percent. Therefore, the two methods produced an average difference in air voids of 0.23 percent.

Table 17: Comparison of Field Samples by Water Absorption Level

Water Absorption Level, %	Air Voids (AASHTO T166), %	Air Voids (Vacuum-Sealing), %	Average Difference, %	t-statistic	p-value	Different?
<0.5	6.43	6.66	0.23	-1.988	0.052	No
0.5 < > 0.75	7.29	7.66	0.37	-1.651	0.110	No
0.75 < > 1.00	7.88	8.00	0.13	-0.346	0.732	No
1.00 < > 1.25	7.75	8.71	0.97	-7.324	0.000	Yes
1.25 < > 1.50	7.20	8.76	1.56	-5.261	0.000	Yes
1.50 < > 1.75	8.16	9.26	1.10	-2.772	0.015	Yes
1.75 < > 2.00	9.03	10.65	1.63	-4.055	0.027	Yes
2.00 < > 2.25	9.86	11.28	1.42	-5.155	0.001	Yes
> 2.25	10.88	13.37	2.50	-8.538	0.000	Yes

The next water absorption level category was from 0.5 to 0.75 percent. A total of 28 cores met this requirement. Results of the paired *t*-tests showed that the two bulk specific gravity methods again produced similar air void contents (Table 17). The average difference in air voids between the two methods was 0.37 percent.

Water absorption levels from 0.75 to 1.00 percent were the next category. Table 17 shows that the two methods again resulted in similar air void contents. The average difference in air voids for this water absorption category was 0.13 percent.

A number of other water absorption level categories were developed on 0.25 percent water absorption increments above 1.00 percent. However, Table 17 shows that the two bulk specific gravity methods resulted in significantly different air void contents once the water absorption level increased above 1.00 percent. This would indicate that the vacuum-sealing method should be utilized when water absorption levels are above 1.00 percent.

An interesting observation about Table 17 is that even at relatively low levels of water absorption (less than 1.00 percent) the vacuum-sealing method provided slightly higher air void contents for each of the water absorption level categories where the two methods were statistically similar. This observation suggests that there could potentially be a small correction factor required in order for the vacuum-sealing method to result in the same air void content as AASHTO T166 for a given sample. Figure 35 illustrates a histogram of the differences in air voids resulting from the vacuum-sealing and AASHTO T166 methods for mixes having water absorption levels less than 0.5 percent water absorption. This figure illustrates that the average difference is above 0.0 and approximately 0.3 percent (as shown in Table 17).

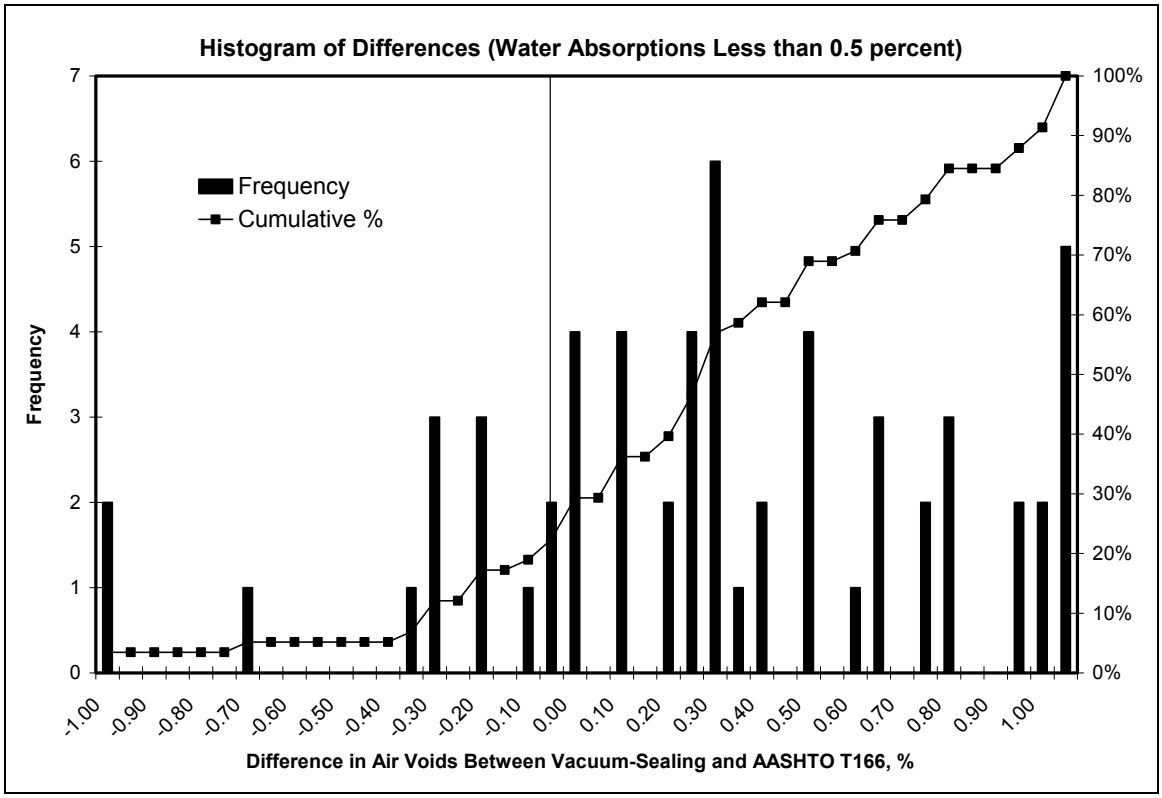

Figure 35: Histogram of Differences in Air Voids for Mixes with Water Absorptions Less than 0.5 Percent

A method of determining a correction factor, if needed, would be to regress water absorption versus the difference in air voids. Figure 36 illustrates the relationship between the difference in air void contents by the vacuum-sealing and AASHTO T166 methods versus water absorption. Based upon the regression equation, the intercept for the data was 0.20 percent air voids. Therefore, 0.20 percent air voids would be subtracted from the vacuum-sealing results in order to match the results from the AASHTO T166 test method.

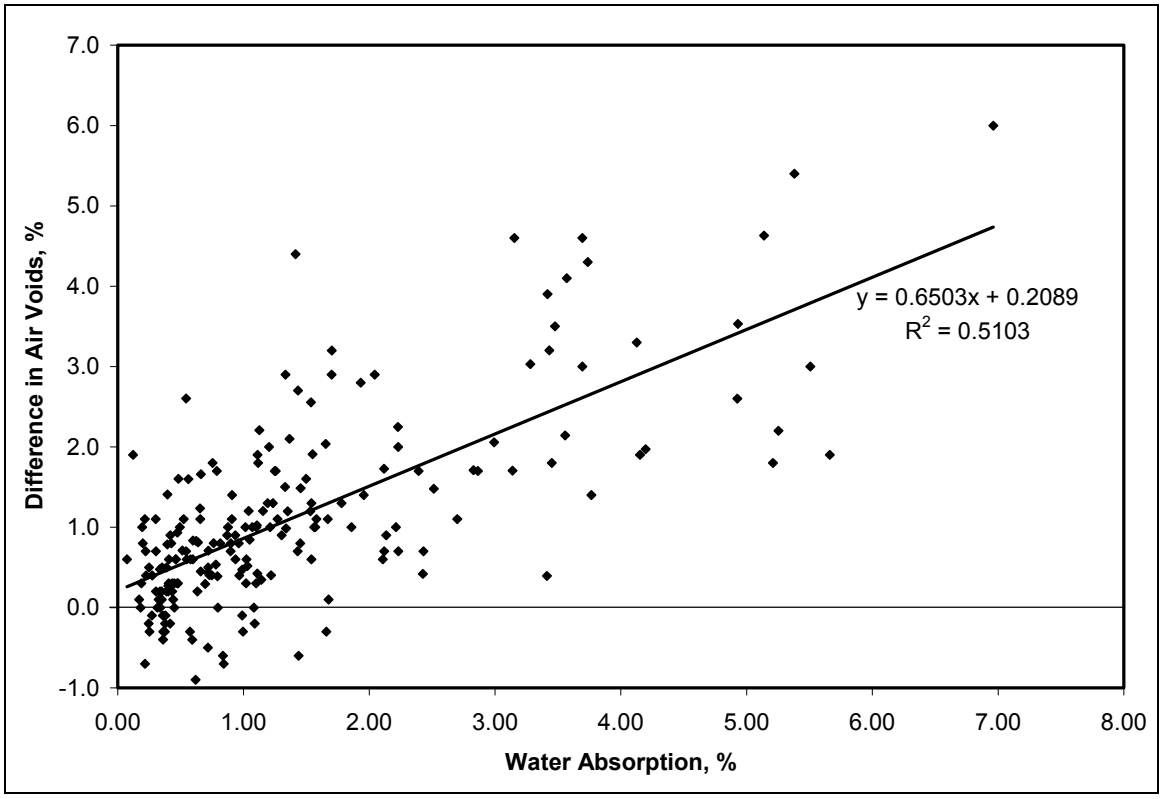

Figure 36: Relationship Between Differences in Air Voids and Water Absorption

There are several factors that could affect a correction factor between the two bulk specific gravity methods; namely, gradation shape and NMAS. The most probable reasons for differences in air void levels (at low water absorption levels) are the surface

texture of samples and the size of individual air voids. Therefore, factors such as gradation shape and NMAS that affect the surface texture and size of air voids would likely affect the correction factor. Thus, if a correction factor is needed, then it would likely be different for each mixture.

7.0 CONCLUSIONS AND RECOMMENDATIONS

The objectives of Task 3, Part 3 were to: (1) compare AASHTO T166 with other methods of measuring bulk specific gravity to determine under what conditions AASHTO T166 is accurate; (2) identify potential improvements to AASHTO T166 to achieve a more accurate measure of bulk specific gravity (if needed); and (3) recommend alternate methods of measuring bulk specific gravity (if needed). Separate sets of data for laboratory prepared samples and field compacted samples were evaluated to accomplish these objectives. Based upon these results the following conclusions are made:

- When laboratory prepared samples having low levels of water absorption were evaluated, the dimensional method resulted in the highest air void contents followed by the gamma ray method. The vacuum-sealing and water displacement (AASHTO T166) methods resulted in similar air void contents when the water absorption level was low.
- At low levels of water absorption, the water displacement method is an accurate measure for bulk specific gravity. The error develops when removing the sample from water to determine the SSD weight. If water flows out of the sample an error occurs. The allowable absorption level to use the displacement test method

is 2% in AASHTO T166 but this level of absorption can create accuracy problems as shown in this report. This number should be reduced to 1% or lower for better accuracy. If the allowable water absorption is reduced much below 1%, many field compacted mixes will exceed this absorption resulting in a need for an alternate test method. It is recommended that the absorption limit for the displacement test method be reduced to 1%. If the vacuum-seal method is adopted on a project the contractor should realize that the compactive effort may now have to be increased over what has been used in the past since the voids measured with the vacuum-seal method will be higher than that measured with the AASHTO T166 method in the 7-10 percent void range or higher.

- The water displacement method was accurate for all water absorption levels encountered for mixes that were fine-graded (ARZ gradations). For mixes having gradations near the maximum density line (TRZ) or coarser (BRZ and SMA), the level of water absorption at which AASHTO T166 was no longer accurate was between 0.2 and 0.4 percent.
- For mix design samples and other laboratory samples that are compacted to relatively low voids, the displacement method will provide reasonable accurate answers. However, for field samples where the void levels will typically be 6% or higher it is important to evaluate absorption to determine if the vacuum-seal method needs to be used.
- Care must be used when using the vacuum sealing method to measure density. Many times the plastic bag developed a leak during the test, leading to an error in the result. Weighing the sample in air after measuring the submerged weight will

indicate if a leak has developed. If a leak is identified the test must be repeated until an acceptable test is achieved.

- There appears to be a need for a correction factor for the vacuum-sealing and water displacement methods to provide equal measured air void contents even when the air void level is low. The correction factor for the mixtures evaluated in this report should be approximately 0.2% air voids. A better determination of the correction factor can be made for specific dense graded mixes by compacting samples in the Superpave gyratory compactor to approximately 4% air voids (design air void content) and testing using the two test methods. The difference between these two tests will be the correction factor for the mix.

8.0 REFERENCES

1. M. S. Buchanan. An Evaluation of Selected Methods for Measuring the Bulk Specific Gravity of Compacted Hot Mix Asphalt (HMA) Mixes. In *Journal of the Association of Asphalt Paving Technologists*, Vol. 69. Reno, NV. 2000. pp. 608-634.

2. Instrotek Incorporated. *Corelok® Operator's Guide*. Version 10, Raleigh, NC. 2001.

3. K. D. Hall, F. T. Griffith, and S. G. Williams. Examination of Operator Variability for Selected Methods for Measuring Bulk Specific Gravity of Hot-Mix Asphalt Concrete. In *Transportation Research Record 1761*, TRB, National Research Council, Washington D. C. 2001.

4. L.A. Cooley, Jr., B.D. Prowell, and M.R. Hainin. "Comparison of the Saturated Surface-Dry and Vacuum Sealing Methods for Determining the Bulk Specific Gravity of Compacted HMA." In *Journal of the Association of Asphalt Paving Technologists*, Vol. 72. Lexington, KY 2003. pp. 56-96.

5. L.A. Cooley, Jr., B.D. Prowell, M.R. Hainin, M.S. Buchanan, and J. Harrington. "Bulk Specific Gravity Round-Robin Using the Corelok Vacuum Sealing Device." FHWA Report No. FHWA-IF-02-044. National Center For Asphalt Technology Report No. 02-11. November 2002.

6. P. Spellerberg, D. Savage, J.Pielert, "Precision Estimates of Selected Volumetric Properties of HMA Using Non-Absorptive Aggregate". Prepared for NCHRP, February 2003.

7. Troxler Electronics Laboratories, Inc. *Manual of Operation and Instruction Model 3660 CoreReader*, Research Triangle Park, NC, 2002.

8. G.A. Malpass and N.P. Khosla,`Evaluation of Gamma Ray Technology for the Direct Measurement of Bulk Specific Gravity of Compacted Asphalt Concrete Mixtures.` In *Journal of the Association of Asphalt Paving Technologists*, Vol. 70. Clearwater Beach, FL 2001. pp. 352-367.

9. J.T. Harvey, Mills, C.Scheffy, J. Sousa and C.L. Monosmith, "An Evaluation of Several Techniques for Measuring Air-Void Content in Asphalt Concrete Specimens." Journal of Testing and Evaluation, JTEVA, Vol. 22, No. 5, September 1994, pp. 424-430.

10. J.E. Stephens, “Bituminous Mix Density By Coated Specimen” University of Connecticut Report No: JHR 73-59, 1973

11. Al-Khaateeb, G., C. Paugh, K. Stuart, T. Harman, and J. D’Angelo. “Target and Tolerance for the Angle of Gyration Used in the Superpave Gyratory Compactor (SGC).” In Transportation Research Record 1789, TRB, National Research Council, Washington, DC. 2002. Pp. 208-215.